Novel insights into surfactant protein C trafficking revealed through the study of a pathogenic mutant

Jennifer A. Dickens[1], Eimear N. Rutherford[1], Susana Abreu[1], Joseph E. Chambers[1], Matthew O. Ellis[1], Annemarie van Schadewijk[2], Pieter S. Hiemstra[2] and Stefan J. Marciniak[1]

[1] Cambridge Institute for Medical Research, Keith Peters Building, Cambridge Biomedical Campus, Cambridge CB2 0XY, UK.
[2] Department of Pulmonology, Leiden University Medical Center, Leiden, Netherlands.

Corresponding author: Jennifer Dickens (jac72@cam.ac.uk)

Abstract

Alveolar epithelial cell (AEC) dysfunction plays an important role in the pathogenesis of idiopathic pulmonary fibrosis (IPF) but remains incompletely understood. Some monogenic forms of pulmonary fibrosis are associated with expression of mutant surfactant protein C (SFTPC). The commonest pathogenic mutant, I73T, mislocalises to the AEC plasma membrane and displays a toxic-gain-of-function. Because the mechanisms explaining the link between this mutant and IPF are incompletely understood, we sought to interrogate SFTPC trafficking in health and disease to understand the functional significance of SFTPC-I73T relocalisation.

We performed mechanistic analysis of SFTPC trafficking in a cell model that reproduces the *in vivo* phenotype and validated findings in human primary alveolar organoids. We show that wild-type SFTPC takes an unexpected indirect trafficking route via the plasma membrane and undergoes the first of multiple cleavage events before reaching the multivesicular body (MVB) for further processing. SFTPC-I73T takes this same route, but its progress is retarded both at the cell surface and due to failure of trafficking into the MVB. Unable to undergo onward trafficking, it is recycled to the plasma membrane as a partially cleaved intermediate.

These data show for the first time that all SFTPC transits the cell surface during normal trafficking, and that the I73T mutation accumulates at the cell surface through both retarded trafficking and active recycling. This understanding of normal SFTPC trafficking and how the I73T mutant disturbs it provides novel insight into SFTPC biology in health and disease, and in the contribution of the SFTPC mutant to IPF development.

Introduction

In idiopathic pulmonary fibrosis (IPF), pathological scarring of the lung impairs gas exchange to cause premature death [1]. Alveolar type 2 (AT2) epithelial cells, the cells that synthesise surfactant and are the progenitors of AT1 cells [2], are crucial in IPF development. It is increasingly recognised that AT2 injury and dysfunction in IPF trigger pathological lung remodelling [3], but limited understanding of the initiating events in IPF has hampered development of therapies that directly modify early pathogenic mechanisms. Familial pulmonary fibrosis (FPF), caused by mutations of individual genes, offers a unique opportunity to examine how specific AT2 defects cause pulmonary fibrosis [4].

Autosomal dominant mutations in surfactant protein C (SFTPC), which is expressed exclusively in AT2 cells, cause FPF. [5]. Expression of the commonest pathogenic variant, SFTPC-I73T [6], can manifest as FPF in childhood or in adults [6] [7]. Some of these variants of SFTPC do not traffic beyond the endoplasmic reticulum (ER) because they are unable to fold correctly. This results in "ER stress" [8], which is seen in the lungs in FPF and sporadic IPF [9]. However, SFTPC-I73T does not cause ER stress, but instead has been reported to mislocalise to the cell surface by unknown mechanisms [10].

Understanding SFTPC trafficking is necessary if we are to explain how the FPF-causing SFTPC-I73T variant causes protein mislocalisation and AT2 dysfunction. SFTPC is produced as a proprotein (proSFTPC) that undergoes several proteolytic steps before being secreted, although surprisingly the location and precise nature of the maturation steps remain unclear. ProSFTPC is a type 2 transmembrane protein that comprises 4 domains (fig 1A): (i) an N-terminal cytosolic domain required for post-Golgi targeting [11] [12] [13] [14]; (ii) a transmembrane helix that forms the mature SFTPC protein [15]; (iii) an unstructured linker domain; and (iv) a C-terminal BRICHOS domain that ensures correct protein folding. Current models suggest that proSFTPC traffics directly from early cellular compartments of the secretory pathway to specialised late endosomes called multivesicular bodies (MVBs), and then to AT2-specific lamellar bodies prior to secretion [16]. *En route*, sequential C- then N-terminal cleavages yield mature SFTPC (fig 1A) [17]. However, the I73T mutation disrupts this process resulting in abnormal accumulation of immature SFTPC at the plasma membrane and in early endosomes [10] [18]. This is reported to have toxic effects on AT2 function, perturbing phospholipid uptake and protein degradation via autophagy and mitophagy [18, 19]. Understanding how the I73T mutation prevents normal trafficking of SFTPC may ultimately enable the development of therapeutics that may prevent AT2 injury and dysfunction, and prevent the onset of fibrosis.

Here, we present a detailed analysis of SFTPC trafficking that shows for the first time that both wild-type and I73T-mutant SFTPC unexpectedly traffic via the plasma membrane. Mislocalisation of SFTPC-I73T results from aberrant recycling of this protein to the cell surface owing to its failure to targeted to the MVB, resulting in its accumulation at the cell surface and recycling endosomes. Our investigation of a rare pathogenic variant thus provides fundamental insights into the biology of SFTPC and the mechanism of disease.

Materials and Methods

Detailed methods including details of chemicals, antibodies, cell lines, siRNAs, CRISPR guides, creation of expression vectors and cell-based assays are available in the supplementary material.

Cell culture

HeLa cells were maintained in DMEM + 10% FBS (+400µg/ml geneticin for stable cell lines). Transfection of DNA was achieved using FuGene 6 (Promega) and clonal transgenic cell lines generated by selection and single cell sorting. Knockout cell pools were generated by liposomal transfection with vectors expressing Cas9, guide RNA, and a fluorescent marker used for fluorescence activated cell sorting (FACS).

Organoid culture

Alveolar organoids were obtained using a feeder-free organoid-based expansion method for tissue-isolated primary alveolar cells. A manuscript describing the details of this method is in preparation (van Riet et al). Briefly, tumour-free peripheral lung tissue was collected from patients undergoing cancer resection and subjected to enzymatic digestion. The use of lung tissue that was collected within the framework of patient care was in line with the "Human Tissue and Medical Research: Code of conduct for responsible use" (2011) (www.federa.org). This code of conduct describes the opt-out system for coded anonymous further use of such samples. Cells were cultured as organoids in Basement Membrane Extract (BME) organoid matrix using feeder-free conditions. Organoids retained AT2 cell characteristics as shown by staining for proSFTPC and HTII-280 and were used at passage 1 for these experiments.

Mouse tissue

Tissue from inducible SFTPC-I73T-expressing mice [18] was a kind gift from Professor Michael Beers.

Unless stated, figures depict representative images from at least 3 independent repeats.

Results

When compared with wild type SFTPC, the I73T variant is mislocalised, misprocessed and aberrantly O-glycosylated

When detected using N-terminal domain (Npro) antibodies, we confirmed that wild-type proSFTPC (hereafter SFTPC-WT) localises to punctate structures consistent with MVBs [20] [21] and that the SFTPC-I73T variant redistributes to the plasma membrane in AT2 cells of SFTPC-I73T transgenic mouse lung (fig 1B) [10, 18].

To investigate the mechanisms responsible, a cell model of early SFTPC trafficking was established. Primary AT2 cells are unsuitable for detailed mechanistic work due to the complexity of genetic manipulation required and their dedifferentiation when grown in monolayer culture [22]. HeLa cells have long been used to undertake studies of protein trafficking and there already exists a large bioresource of genetically altered HeLa lines with which to interrogate the generic biological processes responsible for anterograde trafficking. eGFP-proSFTPC (hereafter GFP-SFTPC) was expressed in HeLa cells where the GFP-tag did not affect localisation compared with untagged proteins (fig s1A). Surface accumulation of GFP-SFTPC-I73T relative to GFP-SFTPC-WT could be detected by microscopy and flow cytometry using an antibody to the BRICHOS domain though interestingly we could detect low levels of SFTPC-WT at the plasma membrane (fig 1C). GFP-SFTPC-I73T also accumulated in tubular structures (fig 1C); which MICAL-L1 and Rab8 co-staining demonstrated to be recycling endosomes (fig s1B).

SFTPC from cell lysates migrated as species of multiple sizes without or with the GFP tag (fig 1D & s1C). GFP-SFTPC-WT migrated as a doublet of ~50kDa and a smaller band at ~34kDa (arrowhead). The doublet represents full-length proSFTPC ± palmitoylation [15, 23]. In keeping with previous studies [10], SFTPC-I73T migrated more slowly and accumulated an additional species "SFTPC*" (*, fig 1D & s1C). Affinity purified GFP-SFTPC-WT and GFP-SFTPC-I73T were subjected to mass spectrometry, which confirmed the upper bands to be full-length protein, whereas the smallest band lacked the BRICHOS domain and linker, and the SFTPC* band in GFP-SFTPC-I73T samples lacked the BRICHOS domain but retained the linker (fig s1D).

To determine the relevance of the I73 residue during SFTPC maturation, a GFP-SFTPC-I73A variant was generated. Like GFP-SFTPC-I73T, this localised to the plasma membrane (fig s2A) and accumulated an SFTPC*-like species (fig s2B). However, bands of GFP-SFTPC-I73A migrated with sizes similar to GFP-SFTPC-WT, albeit in proportions similar to those of GFP-SFTPC-I73T. O-glycosylation frequently occurs on threonine residues of membrane proteins during trafficking [24], so we hypothesised that retardation of SFTPC-I73T might reflect O-glycosylation of T73. This was confirmed by mass spectrometry and by observing that O-glycosidase treatment reverted the migration of GFP-SFTPC-I73T to that of GFP-SFTPC-WT (fig s2C&D).

Mutation of I73 therefore leads to SFTPC accumulation at the cell surface and in recycling endosomes, and promotes accumulation of both uncleaved proSFTPC and the partially processed SFTPC* form, which retains the linker but lacks the BRICHOS domain. This indicates that I73 plays an important role in SFTPC trafficking and proteolysis of its linker region. The observed O-glycosylation of 73T is not responsible for SFTPC mislocation but might plausibly have as yet unstudied toxic effects.

Wild type SFTPC traffics to the plasma membrane

ProSFTPC is believed to traffic directly from the Golgi to an acidic compartment for proteolysis [25] [26]. For direct Golgi to endosome trafficking, cytosolic adaptors (e.g. AP1 or GGA proteins) recognise targeting motifs (e.g. YXXØ or (DE)XXX(LL)) to facilitate packaging into clathrin-coated vesicles [27]. The cytosolic domain of SFTPC lacks such sequences, but GGA proteins (especially GGA2) can recognise some ubiquitinated cargoes lacking targeting sequences [28]. Since SFTPC can be ubiquitinated on lysine 6 (K6), potentially allowing recognition by GGAs, we knocked-down GGA1-3, but detected no effect on GFP-SFTPC localisation or proteolysis (fig s3A&B). However, since gradual depletion of adaptor proteins following knockdown may allow cellular compensation, we next tested the effect of rapid GGA2 inactivation using "knock-sideways" in which GGA2 is relocalised to mitochondria instantaneously upon addition of rapamycin [29]. The "retention using selective hooks" (RUSH) system enabled visualisation of SFTPC trafficking in living cells (fig 2A) [30]. Streptavidin-binding-protein (SBP)-GFP-SFTPC initially localised to the ER, but upon addition of biotin relocalised in patterns resembling GFP-SFTPC (fig 2B). Following biotin-induced release, SBP-GFP-SFTPC-WT trafficked to distal compartments including the plasma membrane, whilst no effect of GGA2-knocksideways was observed (fig s3C&D). This led us to hypothesise that all SFTPC, including wild type, might traffic via the cell surface and not directly from the Golgi to endosomes.

To test this, we compared SFTPC trafficking with that of transferrin receptor (TfnR) and CDMPR, which traffic via the plasma membrane or directly to the endo-lysosomal system respectively (fig 2A) [31]. Strikingly, SFTPC-WT trafficked via tubular post-Golgi structures with TfnR, without colocalisation with CDMPR which exited the Golgi apparatus in vesicles (fig 2C). As expected, SBP-GFP-SFTPC-I73T also trafficked with TfnR then trafficked to the plasma membrane (fig s4A&B) [10]. Remarkably, SBP-GFP-SFTPC-WT also trafficked to the plasma membrane, as visualised by imaging and flow cytometry (fig 2D).

These data show that both SFTPC-WT and SFTPC-I73T traffic directly to the plasma membrane from the Golgi. Thus, the accumulation of SFTPC-I73T at the cell surface represents aberrant retention, rather than mistrafficking *per se*.

SFTPC-WT is retrieved from the plasma membrane by AP2-dependent endocytosis then targeted onwards by K63 oligo-ubiquitination

We next studied the trafficking of SFTPC from the plasma membrane using antibody feeding: cell surface SFTPC was labelled with primary antibody on ice, incubated at 37ºC to allow internalisation, and then remaining cell surface protein detected using a fluorescently-conjugated secondary antibody. Labelled GFP-SFTPC-WT was internalised more completely than GFP-SFTPC-I73T, although there was evidence of some early SFTPC-I73T internalisation (fig 3A). This was unaffected by the fluorescent GFP tags introduced to visualise trafficking (fig s5). The plateauing of the I73T signal may reflect recycling of labelled protein back to the plasma membrane during the course of the assay. The rapidity of initial SFTPC internalisation was consistent with clathrin-mediated endocytosis (CME). Prolonged bafilomycin treatment, which inhibits CME [32], caused accumulation of GFP-SFTPC-WT at the plasma membrane, but had little effect on the distribution of GFP-SFTPC-I73T (fig 3B&C). The involvement of CME was confirmed in AP2-deficient cells, where GFP-SFTPC-WT and GFP-SFTPC-I73T both accumulated at the plasma membrane (fig 3D).

The I73T mutation therefore partially impairs CME despite being topologically unable to interact with sorting factors such as AP2. Many membrane proteins undergo clustering to promote CME. Indeed,

oligomerisation of SFTPC is known to occur during its trafficking [20]. However, immunoprecipitation of co-expressed GFP-SFTPC and HA-SFTPC yielded hetero-oligomers of both SFTPC-WT and SFTPC-I73T, suggesting that impaired endocytosis of SFTPC-I73T is unlikely to be explained by failure of oligomerisation (fig 4A).

We next considered the possibility that aberrant ubiquitination of SFTPC-I73T contributes to disrupted trafficking. SFTPC is ubiquitinated on residue K6, which has been reported to be involved in endosomal targeting [13, 14]. Immunoprecipitation of untagged and GFP-tagged SFTPC confirmed oligo-ubiquitination of SFTPC-WT that was absent in SFTPC-I73T (fig 4B&s6A). We generated GFP-SFTPC-K6R and confirmed this was not ubiquitinated (fig s6B). However, the rate of SFTPC-K6R internalisation was indistinguishable from that of SFTPC-WT indicating that ubiquitination is unnecessary for endocytosis and therefore cannot account for differing rates of endocytosis between SFTPC-WT and SFTPC-I73T (fig 4C&s5).

The observed accumulation of SFTPC-I73T in recycling endosomes suggests failure of sorting at endosomes towards MVBs. By microscopy, we observed that ubiquitination-deficient GFP-SFTPC-K6R localised to the plasma membrane and recycling endosomes (fig 5A and s6C). Since internalisation of proteins into intraluminal vesicles of MVBs involves recognition of ubiquitinated cargo by the ESCRT machinery [33], we depleted cells of ESCRT0 protein Hrs [34] and observed a dramatic relocalisation of GFP-SFTPC-WT to recycling endosomes and the plasma membrane (fig 5B). K63 chains of ubiquitin generated by the E2-ligase (Ube2N) [35] mark proteins for trafficking to endosomes [33]. When Ube2N was depleted, GFP-SFTPC-WT again redistributed to recycling endosomes and the plasma membrane (fig 5C).

These results demonstrate that both SFTPC-WT and SFTPC-I73T are endocytosed in an AP2-dependent manner, although SFTPC-I73T is internalised less efficiently. K63 ubiquitination of SFTPC-WT then directs it to MVB intraluminal vesicles. Failure of this sorting event redirects SFTPC-I73T to the plasma membrane via recycling endosomes.

SFTPC undergoes C-terminal cleavage following endocytosis prior to entering the MVB

Proteolytic maturation of SFTPC occurs in acidic post-Golgi compartments [25, 36]. A cathepsin H-mediated N-terminal cleavage in MVBs [26] is preceded by C-terminal cleavages at an unknown location. Cleavage events occurring before MVB entry can be studied in HeLa cells whereas assessment of N-terminal proteolysis in later compartments requires the presence of all SFTPC trafficking compartments (including lamellar bodies) and was therefore not studied further here.

Using the RUSH system, we observed at 30 min following ER release, full-length SFTPC-WT and SFTPC-I73T both underwent palmitoylation giving rise to a slower migrating band visualised by immunoblot (fig 6A). From 3 hours, full-length SFTPC-WT was lost whilst a 37kDa C-terminally cleaved product appeared (arrowhead). In contrast, more full-length SFTPC-I73T was retained and the SFTPC* product accumulated. A similar band was observed early in SFTPC-WT-expressing cells, but disappeared by 3 hours. We conclude that early C-terminal proteolysis generating SFTPC* occurs in a compartment accessible to both SFTPC-WT and SFTPC-I73T. The selective accumulation of SFTPC* with SFTPC-I73T expression suggests that sequential C-terminal processing is impaired by I73T. To determine if this is a cause or consequence of aberrant trafficking, we deleted Ube2N or depleted ESCRT0 protein Hrs to impair MVB import. Both caused WT-SFTPC* to accumulate suggesting that access to MVBs is necessary for the final C-terminal cleavage (fig 6B). The persistence of low levels

of C-terminally-cleaved SFTPC in all conditions, suggests an incomplete trafficking block or some redundancy in SFTPC sorting.

To determine the subcellular location of C-terminal proteolysis, we generated GFP-SFTPC-WT-HaloTag and confirmed its correct trafficking and cleavage (fig s7). The majority of GFP-SFTPC-WT-HaloTag-containing puncta retained both tags, identifying them as compartments prior to C-terminal proteolysis (fig 6C). In AP2 deficient cells, uncleaved GFP-SFTPC-WT-HaloTag accumulated at the plasma membrane, indicating that full-length SFTPC first reaches the cell surface and undergoes C-terminal proteolysis following endocytosis. This finding is further supported by the observation that bafilomycin-mediated inhibition of endocytosis results in accumulation of full length proSFTPC but has a relatively smaller effect on the abundance of the * intermediate (fig 6D).

We sought to determine if impaired C-terminal proteolysis contributes to mislocalisation of SFTPC-I73T or is a consequence. Flow cytometric detection of cell-surface BRICHOS domain (uncleaved protein) had shown less dramatic differences between SFTPC-WT and SFTPC-I73T than were observed by imaging the cytosolic GFP-tag (fig 1C). Similar results had been obtained when SFTPC-WT was redistributed to the cell surface by impairing endosomal sorting (fig 5B&C). This suggested that recycled SFTPC might undergo C-terminal proteolysis prior to recycling. To investigate this, we treated intact cells with proteinase K to digest surface-exposed proteins (fig 6E). HLA served as a control for surface-exposure, while GAPDH reported cytosolic proteolysis. Full-length SFTPC-WT and SFTPC-I73T were digested by low concentrations of proteinase K similar to those required for HLA digestion confirming their presence at the cell surface. The fully C-terminally-cleaved 37kDa band, by contrast, resisted proteolysis to a similar extent as GAPDH suggesting an intracellular localisation. SFTPC* showed an intermediate sensitivity to proteinase K, consistent with a mixed surface and endosomal localisation. As the proteinase K digestion was performed on ice, no trafficking of SFTPC could occur during this incubation. Consequently, loss of the SFTPC* intermediate reflects its digestion by proteinase K, rather than being an indirect effect of losing full-length proSFTPC.

Full-length SFTPC is therefore first trafficked to the cell surface and then, following AP2-dependent endocytosis, C-terminal proteolysis occurs distal to the linker domain to yield SFTPC*. This is followed by a juxta-membrane cleavage to generate fully C-terminally-cleaved SFTPC. While SFTPC-WT is then rapidly transported to the MVB for N-terminal proteolysis, the I73T mutation impairs juxta-membrane cleavage leading to recycling of SFTPC* to the cell surface.

SFTPC cleavage is necessary for targeting away from the cell surface to MVBs

We wished to determine if proteolytic removal of the linker region serves as a signal to divert SFTPC to MVBs and away from recycling to the plasma membrane. Another BRICHOS-domain-containing protein, Bri2, undergoes sequential cleavage first by furin distant from the membrane and then closer to the membrane by the membrane-bound sheddase ADAM10 [37]. Our attempts to insert tags between the transmembrane domain and linker impaired juxta-membrane cleavage especially with longer tags (fig s8). This disproportionately affected SFTPC-WT leading to accumulation of an SFTPC*-like product. Suspecting that juxta-membrane cleavage might be mediated by an endosomal membrane-bound sheddase, we treated cells with Z-VLL-CHO, an inhibitor of such proteases. Z-VLL-CHO dramatically increased levels of SFTPC-WT in lysates, predominantly as full-length protein and BRICHOS-cleaved intermediates (fig 7A) with accumulation of SFTPC-WT at the cell surface (fig 7B&C). Proteolytic processing of SFTPC-I73T was further impaired by Z-VLL-CHO, and SFTPC-I73T remained at the cell surface.

Since SFTPC is expressed exclusively in AT2 cells, it was necessary to validate these findings in a physiologically relevant model. We therefore generated organoids from primary AT2 cells isolated from human lungs. These lung organoids were composed of polarised AT2 cells with apical membranes directed towards the lumen. Immunofluorescence demonstrated endogenous SFTPC-WT in punctate structures beneath the apical surface, while treatment with either bafilomycin (to inhibit CME) or Z-VLL-CHO (to inhibit endosomal sheddases) redistributed endogenous proSFTPC into AT2 apical membranes (fig 8A). These findings align with the trafficking route mechanistically explored in HeLa cells.

Taken together, these experiments reveal that SFTPC undergoes proteolysis distal to the linker domain in endosomes followed by juxta-membrane cleavage, likely by a membrane-bound sheddase. Impaired juxta-membrane cleavage, either induced pharmacologically or by the I73T mutation, results in unproductive recycling of SFTPC between endosomes and the plasma membrane (fig 8B).

Discussion

We set out to understand the mechanisms by which SFTPC-I73T mistraffics to provide insight into its role in FPF. In doing so, we have defined the itinerary of wild-type SFTPC, which involves trafficking via the plasma membrane. We observed that residue I73 of SFTPC, located within the extracellular linker region of the proprotein, is key to trafficking as its mutation results in impaired progression to MVBs and unproductive SFTPC recycling between the cell surface and early endosomes.

Aberrant retention of the linker region is associated with failure of SFTPC ubiquitination, which does not affect endocytosis but impairs subsequent internalisation of SFTPC into MVBs. Our work delineates a mechanism that explains the previous observation that SFTPC-I73T localises to early endosomes while wild type protein is found in MVBs [6]. The precise mechanism though which linker cleavage results in MVB targeting of wild-type SFTPC remains unclear, but linker proteolysis may be necessary to facilitate sorting into late endosomes and/or enables K63-ubiquitination. The partial block of trafficking of SFTPC-I73T seen both in cultured cells and in SFTPC-I73T transgenic mice [18], suggests that I73T produces an incomplete block on trafficking and maturation of the protein.

SFTPC is a highly hydrophobic protein thought to promote the spreading of pulmonary surfactant through interaction with phospholipid layers [17]. How SFTPC mutations cause familial pulmonary fibrosis is unclear. Mice lacking SFTPC are viable and grow normally [38], while conditional expression of pathogenic SFTPC mutants results in pulmonary fibrosis [18] [39]. This suggests that the pathogenic mechanism is one of toxic gain-of-function mediated by an abnormal protein rather than loss of function due to SFTPC deficiency. While mutations of the BRICHOS domain causes ER stress [40, 41], the toxic mechanism of linker region mutants is unclear.

Here, we demonstrate that SFTPC-I73T accumulates at the plasma membrane through abnormal recycling from endosomes and from impaired internalisation. Recycled SFTPC-I73T includes the partially cleaved intermediate SFTPC*, consistent with previous plasma membrane profiling data [19]. Interestingly, such abnormal C-terminal SFTPC fragments are present in the bronchoalveolar lavage fluid of individuals with the SFTPC-I73T mutation [6, 42]. Those observations, together with our findings, collectively suggest that C-terminal cleavage products are released into the extracellular space during aberrant recycling of SFTPC. It is tempting to speculate that trafficking of SFTPC-WT via the cell surface may have a role in normal AT2 cell function that is perturbed by the I73T mutant. Ongoing work will determine if surface accumulation of SFTPC in its multiple forms, retention in recycling endosomes and/or the released C-terminal cleavage products themselves affect signalling within the AT2 cell or with its neighbours. Understanding the intracellular interactome of SFTPC and its processing intermediates may shed fresh light on this. Alternatively, saturation of protein recycling pathways by SFTPC might have deleterious effects on surface expression of otherwise unrelated proteins.

In this work, by studying a naturally occurring pathogenic variant of SFTPC associated with FPF, we have discovered that all wild type protein traffics via the cell surface to MVBs, rather than directly from the Golgi. The accumulation of the SFTPC-I73T variant at the plasma membrane therefore reflects retardation along its normal route rather than mistrafficking *per se*. Whether SFTPC possesses additional functions that require it to transit via the cell surface remains to be established, and may prove crucial in understanding the role of SFTPC-I73T in alveolar dysfunction resulting in FPF. Such insight may also help to clarify the role of alveolar dysfunction in other, non-familial forms of IPF.

Acknowledgements

The authors would like to thank Prof. Margaret Robinson, Prof. Matthew Seaman, Prof. Paul Lehner, Dr. David Gershlick and Dr. James Edgar (University of Cambridge, UK), Dr. Anne van der Does (Department of Pulmonology, Leiden University Medical Center, Netherlands) and Prof. Michael Beers (University of Pennsylvania) for helpful advice and reagents.

References

1. Hutchinson J, Fogarty A, Hubbard R, McKeever T. Global incidence and mortality of idiopathic pulmonary fibrosis: a systematic review. *Eur Respir J* 2015: 46(3): 795-806.
2. Desai TJ, Brownfield DG, Krasnow MA. Alveolar progenitor and stem cells in lung development, renewal and cancer. *Nature* 2014: 507(7491): 190-194.
3. Selman M, Pardo A. Revealing the pathogenic and aging-related mechanisms of the enigmatic idiopathic pulmonary fibrosis. an integral model. *Am J Respir Crit Care Med* 2014: 189(10): 1161-1172.
4. Kropski JA, Blackwell TS, Loyd JE. The genetic basis of idiopathic pulmonary fibrosis. *Eur Respir J* 2015: 45(6): 1717-1727.
5. Nogee LM, Dunbar AE, 3rd, Wert S, Askin F, Hamvas A, Whitsett JA. Mutations in the surfactant protein C gene associated with interstitial lung disease. *Chest* 2002: 121(3 Suppl): 20S-21S.
6. Brasch F, Griese M, Tredano M, Johnen G, Ochs M, Rieger C, Mulugeta S, Muller KM, Bahuau M, Beers MF. Interstitial lung disease in a baby with a de novo mutation in the SFTPC gene. *Eur Respir J* 2004: 24(1): 30-39.
7. van Moorsel CH, van Oosterhout MF, Barlo NP, de Jong PA, van der Vis JJ, Ruven HJ, van Es HW, van den Bosch JM, Grutters JC. Surfactant protein C mutations are the basis of a significant portion of adult familial pulmonary fibrosis in a dutch cohort. *Am J Respir Crit Care Med* 2010: 182(11): 1419-1425.
8. Dickens JA, Malzer E, Chambers JE, Marciniak SJ. Pulmonary endoplasmic reticulum stress-scars, smoke, and suffocation. *FEBS J* 2019: 286(2): 322-341.
9. Korfei M, Ruppert C, Mahavadi P, Henneke I, Markart P, Koch M, Lang G, Fink L, Bohle RM, Seeger W, Weaver TE, Guenther A. Epithelial endoplasmic reticulum stress and apoptosis in sporadic idiopathic pulmonary fibrosis. *Am J Respir Crit Care Med* 2008: 178(8): 838-846.
10. Beers MF, Hawkins A, Maguire JA, Kotorashvili A, Zhao M, Newitt JL, Ding W, Russo S, Guttentag S, Gonzales L, Mulugeta S. A nonaggregating surfactant protein C mutant is misdirected to early endosomes and disrupts phospholipid recycling. *Traffic* 2011: 12(9): 1196-1210.
11. Conkright JJ, Bridges JP, Na CL, Voorhout WF, Trapnell B, Glasser SW, Weaver TE. Secretion of surfactant protein C, an integral membrane protein, requires the N-terminal propeptide. *J Biol Chem* 2001: 276(18): 14658-14664.
12. Johnson AL, Braidotti P, Pietra GG, Russo SJ, Kabore A, Wang WJ, Beers MF. Post-translational processing of surfactant protein-C proprotein: targeting motifs in the NH(2)-terminal flanking domain are cleaved in late compartments. *Am J Respir Cell Mol Biol* 2001: 24(3): 253-263.
13. Kotorashvili A, Russo SJ, Mulugeta S, Guttentag S, Beers MF. Anterograde transport of surfactant protein C proprotein to distal processing compartments requires PPDY-mediated association with Nedd4 ubiquitin ligases. *J Biol Chem* 2009: 284(24): 16667-16678.
14. Conkright JJ, Apsley KS, Martin EP, Ridsdale R, Rice WR, Na CL, Yang B, Weaver TE. Nedd4-2-mediated ubiquitination facilitates processing of surfactant protein-C. *Am J Respir Cell Mol Biol* 2010: 42(2): 181-189.
15. Curstedt T, Johansson J, Persson P, Eklund A, Robertson B, Lowenadler B, Jornvall H. Hydrophobic surfactant-associated polypeptides: SP-C is a lipopeptide with two palmitoylated cysteine residues, whereas SP-B lacks covalently linked fatty acyl groups. *Proc Natl Acad Sci U S A* 1990: 87(8): 2985-2989.

16. Kabore AF, Wang WJ, Russo SJ, Beers MF. Biosynthesis of surfactant protein C: characterization of aggresome formation by EGFP chimeras containing propeptide mutants lacking conserved cysteine residues. *J Cell Sci* 2001: 114(Pt 2): 293-302.
17. Whitsett JA, Weaver TE. Hydrophobic surfactant proteins in lung function and disease. *N Engl J Med* 2002: 347(26): 2141-2148.
18. Nureki SI, Tomer Y, Venosa A, Katzen J, Russo SJ, Jamil S, Barrett M, Nguyen V, Kopp M, Mulugeta S, Beers MF. Expression of mutant Sftpc in murine alveolar epithelia drives spontaneous lung fibrosis. *J Clin Invest* 2018: 128(9): 4008-4024.
19. Hawkins A, Guttentag SH, Deterding R, Funkhouser WK, Goralski JL, Chatterjee S, Mulugeta S, Beers MF. A non-BRICHOS SFTPC mutant (SP-CI73T) linked to interstitial lung disease promotes a late block in macroautophagy disrupting cellular proteostasis and mitophagy. *Am J Physiol Lung Cell Mol Physiol* 2015: 308(1): L33-47.
20. Wang WJ, Russo SJ, Mulugeta S, Beers MF. Biosynthesis of surfactant protein C (SP-C). Sorting of SP-C proprotein involves homomeric association via a signal anchor domain. *J Biol Chem* 2002: 277(22): 19929-19937.
21. Kobayashi T, Vischer UM, Rosnoblet C, Lebrand C, Lindsay M, Parton RG, Kruithof EK, Gruenberg J. The tetraspanin CD63/lamp3 cycles between endocytic and secretory compartments in human endothelial cells. *Mol Biol Cell* 2000: 11(5): 1829-1843.
22. Mao P, Wu S, Li J, Fu W, He W, Liu X, Slutsky AS, Zhang H, Li Y. Human alveolar epithelial type II cells in primary culture. *Physiol Rep* 2015: 3(2).
23. Vorbroker DK, Dey C, Weaver TE, Whitsett JA. Surfactant protein C precursor is palmitoylated and associates with subcellular membranes. *Biochim Biophys Acta* 1992: 1105(1): 161-169.
24. Van den Steen P, Rudd PM, Dwek RA, Opdenakker G. Concepts and principles of O-linked glycosylation. *Crit Rev Biochem Mol Biol* 1998: 33(3): 151-208.
25. Beers MF, Kim CY, Dodia C, Fisher AB. Localization, synthesis, and processing of surfactant protein SP-C in rat lung analyzed by epitope-specific antipeptide antibodies. *J Biol Chem* 1994: 269(32): 20318-20328.
26. Brasch F, Ten Brinke A, Johnen G, Ochs M, Kapp N, Muller KM, Beers MF, Fehrenbach H, Richter J, Batenburg JJ, Buhling F. Involvement of cathepsin H in the processing of the hydrophobic surfactant-associated protein C in type II pneumocytes. *Am J Respir Cell Mol Biol* 2002: 26(6): 659-670.
27. Hinners I, Tooze SA. Changing directions: clathrin-mediated transport between the Golgi and endosomes. *J Cell Sci* 2003: 116(Pt 5): 763-771.
28. Scott PM, Bilodeau PS, Zhdankina O, Winistorfer SC, Hauglund MJ, Allaman MM, Kearney WR, Robertson AD, Boman AL, Piper RC. GGA proteins bind ubiquitin to facilitate sorting at the trans-Golgi network. *Nat Cell Biol* 2004: 6(3): 252-259.
29. Hirst J, Borner GH, Antrobus R, Peden AA, Hodson NA, Sahlender DA, Robinson MS. Distinct and overlapping roles for AP-1 and GGAs revealed by the "knocksideways" system. *Curr Biol* 2012: 22(18): 1711-1716.
30. Boncompain G, Divoux S, Gareil N, de Forges H, Lescure A, Latreche L, Mercanti V, Jollivet F, Raposo G, Perez F. Synchronization of secretory protein traffic in populations of cells. *Nat Methods* 2012: 9(5): 493-498.
31. Chen Y, Gershlick DC, Park SY, Bonifacino JS. Segregation in the Golgi complex precedes export of endolysosomal proteins in distinct transport carriers. *J Cell Biol* 2017: 216(12): 4141-4151.
32. Kozik P, Hodson NA, Sahlender DA, Simecek N, Soromani C, Wu J, Collinson LM, Robinson MS. A human genome-wide screen for regulators of clathrin-coated vesicle formation reveals an unexpected role for the V-ATPase. *Nat Cell Biol* 2013: 15(1): 50-60.

33. Shields SB, Piper RC. How ubiquitin functions with ESCRTs. *Traffic* 2011: 12(10): 1306-1317.
34. Ren X, Hurley JH. VHS domains of ESCRT-0 cooperate in high-avidity binding to polyubiquitinated cargo. *EMBO J* 2010: 29(6): 1045-1054.
35. Hofmann RM, Pickart CM. In vitro assembly and recognition of Lys-63 polyubiquitin chains. *J Biol Chem* 2001: 276(30): 27936-27943.
36. Beers MF. Inhibition of cellular processing of surfactant protein C by drugs affecting intracellular pH gradients. *J Biol Chem* 1996: 271(24): 14361-14370.
37. Martin L, Fluhrer R, Reiss K, Kremmer E, Saftig P, Haass C. Regulated intramembrane proteolysis of Bri2 (Itm2b) by ADAM10 and SPPL2a/SPPL2b. *J Biol Chem* 2008: 283(3): 1644-1652.
38. Glasser SW, Burhans MS, Korfhagen TR, Na CL, Sly PD, Ross GF, Ikegami M, Whitsett JA. Altered stability of pulmonary surfactant in SP-C-deficient mice. *Proc Natl Acad Sci U S A* 2001: 98(11): 6366-6371.
39. Katzen J, Wagner BD, Venosa A, Kopp M, Tomer Y, Russo SJ, Headen AC, Basil MC, Stark JM, Mulugeta S, Deterding RR, Beers MF. An SFTPC BRICHOS mutant links epithelial ER stress and spontaneous lung fibrosis. *JCI Insight* 2019: 4(6).
40. Nogee LM, Dunbar AE, 3rd, Wert SE, Askin F, Hamvas A, Whitsett JA. A mutation in the surfactant protein C gene associated with familial interstitial lung disease. *N Engl J Med* 2001: 344(8): 573-579.
41. Wang WJ, Mulugeta S, Russo SJ, Beers MF. Deletion of exon 4 from human surfactant protein C results in aggresome formation and generation of a dominant negative. *J Cell Sci* 2003: 116(Pt 4): 683-692.
42. Galetskiy D, Woischnik M, Ripper J, Griese M, Przybylski M. Aberrant processing forms of lung surfactant proteins SP-B and SP-C revealed by high-resolution mass spectrometry. *Eur J Mass Spectrom (Chichester)* 2008: 14(6): 379-390.

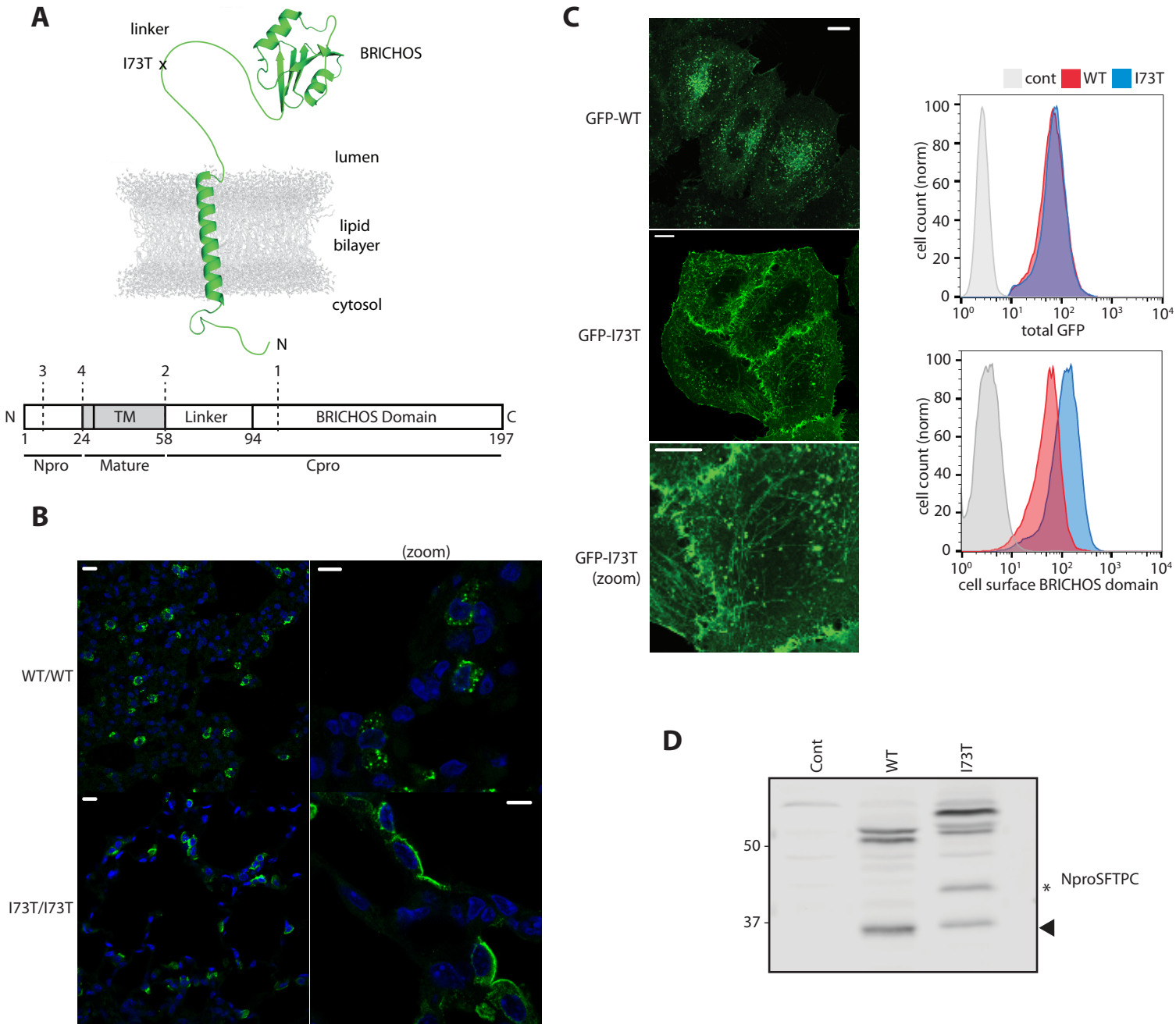

Fig 1. SFTPC-I73T is aberrantly located and processed *in vivo* and *in vitro*. (A) Schematics of SFTPC delineating structure and location of the pathogenic I73T mutation along with domains and approximate reported cleavage sites (dashed lines, numbered 1-4). (B) ProSFTPC immunostaining of alveolar tissue from transgenic mice conditionally expressing SFTPC-WT or SFTPC-I73T reveal punctate intracellular staining of SFTPC-WT and redistribution of SFTPC-I73T to the apical plasma membrane. (C) When GFP-SFTPC-WT is expressed in HeLa cells it localises in intracellular punctate structures, whereas GFP-SFTPC-I73T relocalises to the plasma membrane and intracellular tubular structures. In cells expressing equal amounts of GFP (upper right panel), there is an excess of cell surface SFTPC-I73T as measured by a BRICHOS domain antibody (lower right panel). (D) Immunoblotting of lysates from vector control or GFP-SFTPC expressing cells using an NproSFTPC antibody reveal altered processing of SFTPC-I73T. TM = transmembrane. Scale bar = 10μm / 5μm (zoomed images).

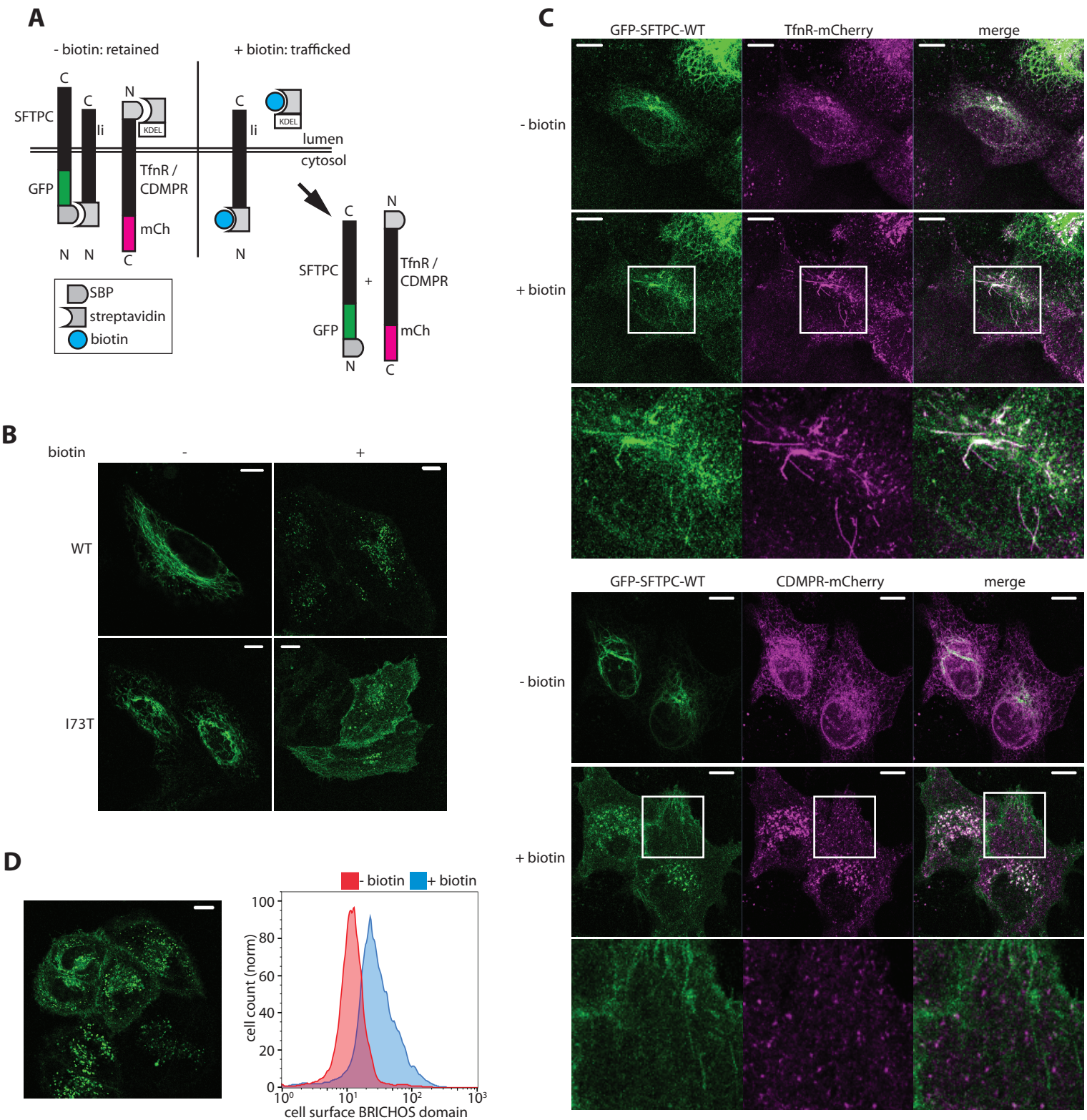

Fig 2. All SFTPC is trafficked from early compartments to the plasma membrane. (A) Schematic of RUSH system in which proteins are held in early trafficking compartments using a streptavidin "hook" before release after addition of biotin. SBP = streptavidin binding protein. (B) Localisation of SFTPC in HeLa cells expressing the RUSH-GFP-SFTPC fusion protein treated ± biotin for 16 hours confirms they traffic normally to post-Golgi compartments. (C) Real-time trafficking of GFP-SFTPC with TfnR or CDMPR reveal co-localisation of SFTPC with TfnR in tubular structures but failure of co-localisation beyond the Golgi with CDMPR which is seen in vesicles. (D) After 2 hours of biotin exposure, GFP-SFTPC-WT is visible at the plasma membrane; this is reflected in increased BRICHOS domain presence at the plasma membrane by flow cytometry. Scale bar = 10μm.

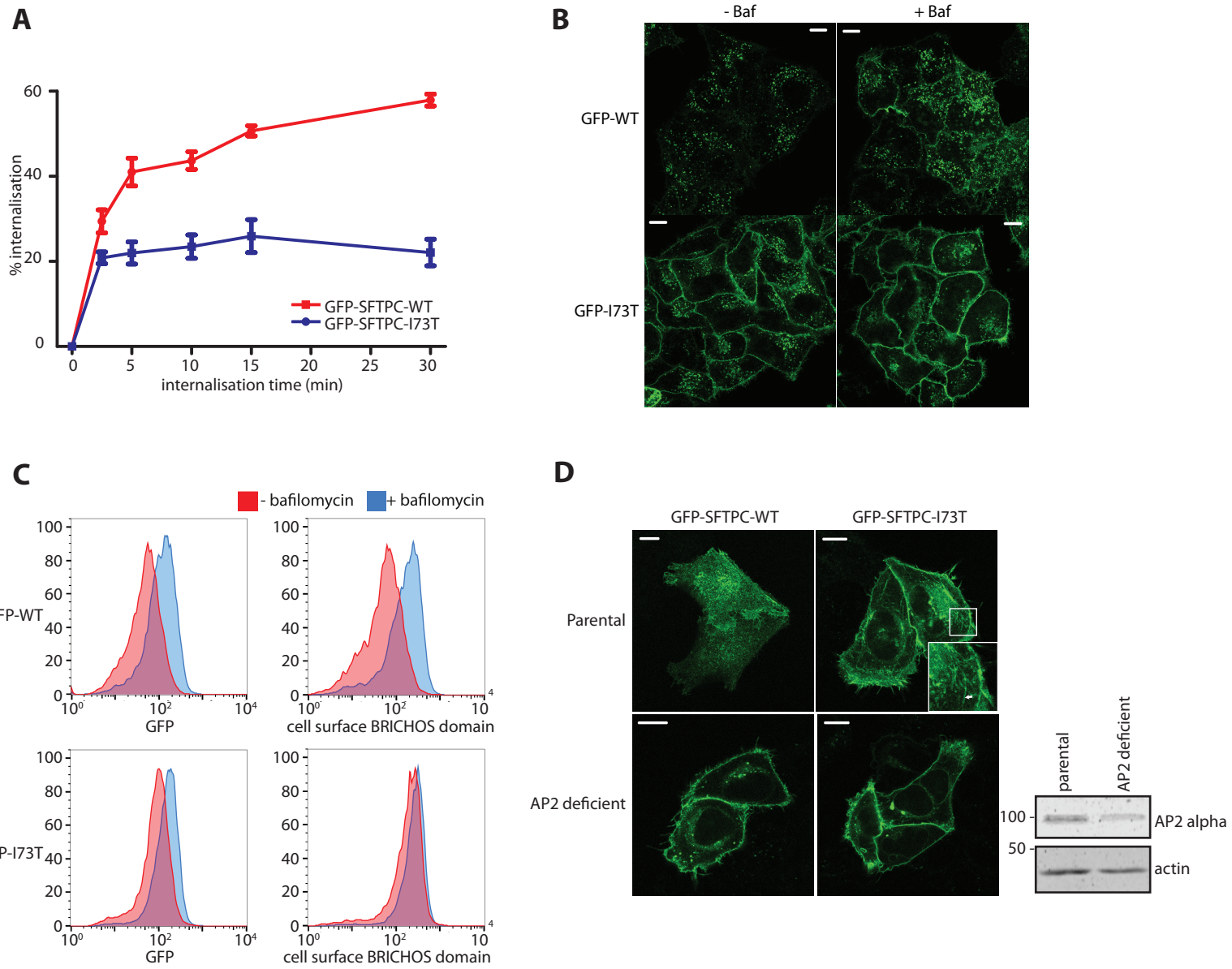

Fig 3. SFTPC internalisation from the plasma membrane is AP-2 dependent and is retarded by the I73T mutation. (A) Quantitative SFTPC internalisation assay. Cells expressing GFP-SFTPC-WT or I73T were labelled with a BRICHOS domain antibody on ice, then protein allowed to internalise at 37°C for the indicated times. Cells were placed back on ice, fixed but not permeabilised, and labelled with a secondary antibody before analysis by flow cytometry. n=3, mean +/- sem. (B and C) HeLa cells stably expressing GFP-SFTPC-WT or I73T were treated with 30μM bafilomycin for 16 hours to inhibit clathrin-mediated endocytosis. This results in cell surface SFTPC accumulation as seen by confocal microscopy and measured by flow cytometry. (D) AP2 deficient cells were used to assess localisation of RUSHed GFP-SFTPC-WT and I73T after 2 hours of biotin treatment. AP2M1 CRISPR knockout cells were immunoblotted for the AP2 alpha subunit. Although some alpha subunit remains, this complex is non-functional. Scale bar = 10μm.

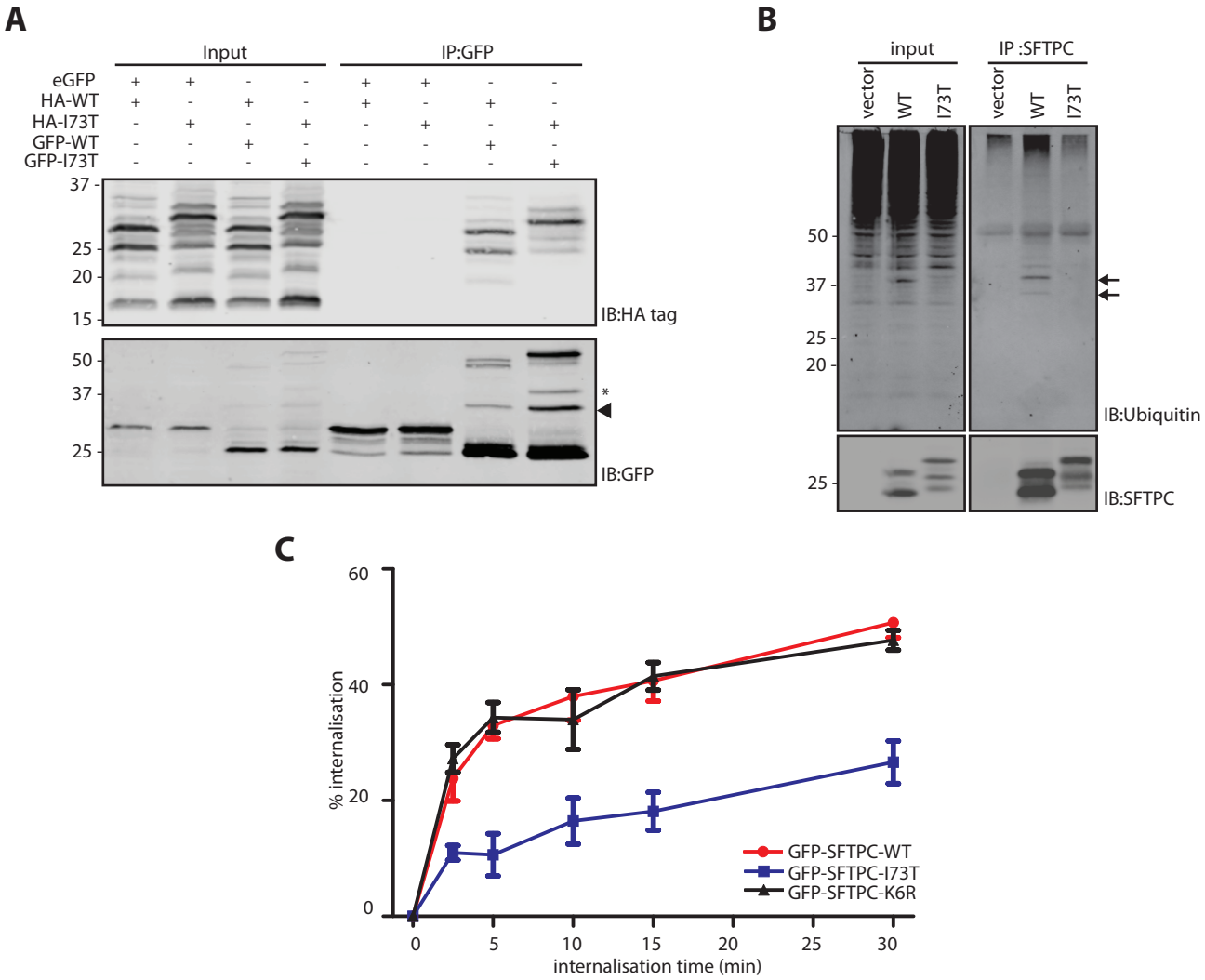

Fig 4. Retardation of SFTPC-I73T internalisation is not due to failed oligomerisation or ubiquitination. (A) HeLa cells were transfected with HA-tagged and GFP-tagged SFTPC (WT or I73T) and lysates subjected to anti-GFP immunoprecipitation before immunoblotting for the HA tag and GFP. Both SFTPC-WT and SFTPC-I73T are equally able to oligomerise. (B) Lysates from HeLa cells expressing SFTPC-WT or SFTPC-I73T were subjected to SFTPC immunoprecipitation and immunoblotted for ubiquitin. Note the presence of oligoubiquitinated SFTPC-WT (arrows) which is not seen in I73T-expressing cells. (C) Quantitative SFTPC internalisation assay of cells expressing GFP-SFTPC-WT, I73T or K6R. n=3, mean +/- sem.

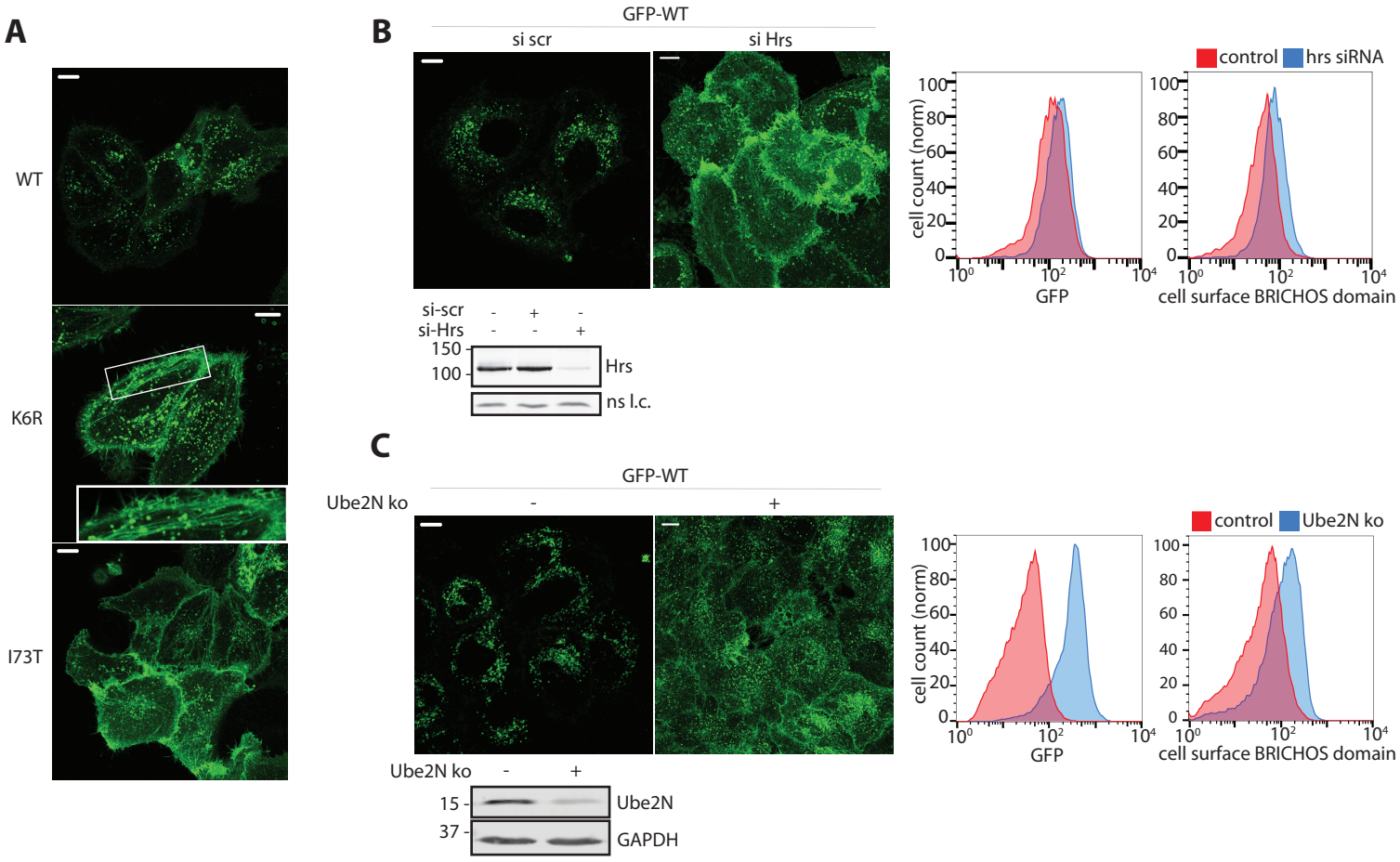

Fig 5. SFTPC ubiquitination in K63 chains is required for trafficking into MVBs. (A) Confocal imaging of HeLa cells expressing GFP-SFTPC-WT, ubiquitination-deficient K6R and I73T reveals that like I73T, SFTPC-K6R is redistributed to the cell surface and into recycling endosomes (middle panel, inset). (B) HeLas were transfected with either scrambled (scr) or ESCRT0 protein Hrs siRNA for 48 hours. Immunoblotting confirmed knockdown and confocal imaging revealed dramatic redistribution of GFP-SFTPC-WT to the plasma membrane. Flow cytometry confirmed a slight increase in total GFP plus partial redistribution of SFTPC to the plasma membrane in the presence of hrs siRNA. (C) A Ube2N CRISPR knockout pool was made and success confirmed by immunoblot. Confocal microscopy revealed both an overall increase in GFP signal along with redistribution of GFP-SFTPC-WT to the plasma membrane in these cells, confirmed by flow cytometry. Scale bar = 10μm.

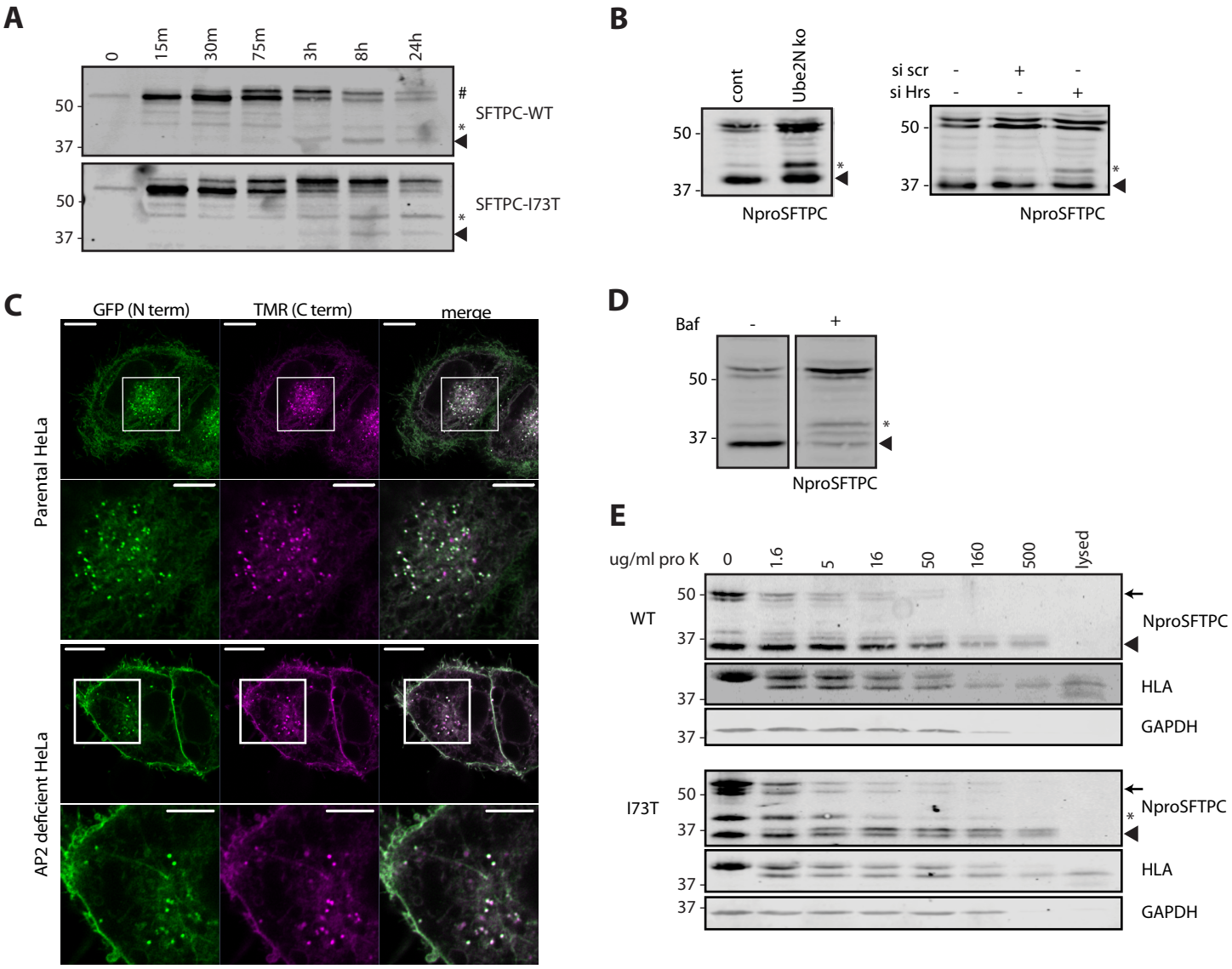

Fig 6. SFTPC C terminal cleavage occurs after transit via the plasma membrane but prior to MVB internalisation. (A) HeLa cells expressing the RUSH-SFTPC fusion protein were allowed to traffic for the times indicated before lysates were subjected to GFP immunoprecipitation and NproSFTPC immunoblotting. The intermediate forms appear contemporaneously for SFTPC-WT and I73T but the first I73T intermediate accumulates as the WT intermediate is cleared. (B) HeLa cells deficient in Uben2N or Hrs in which SFTPC cannot enter MVBs accumulate SFTPC*. (C) HeLa cells were transfected with GFP-SFTPC-Halo and the Halotag labelled with TMR ligand for 15 minutes before fixing. (D) Treatment of GFP-SFTPC-WT expressing HeLa cells with 100nM bafilomycin for 16hrs results in preferential accumulation of full length proprotein. (E) HeLa cells stably expressing GFP-SFTPC-WT or I73T were incubated with proteinase K to digest exposed proteins at the plasma membrane before being lysed and subjected to immunoblot for SFTPC, HLA and GAPDH. The full length (WT and I73T) and intermediate (SFTPC*) species are digested by proteinase K, suggesting they reside at least partially at the cell surface. (Lysed = lysis before proteinase K treatment). Scale bar = 10μm / 5μm (zoomed images).

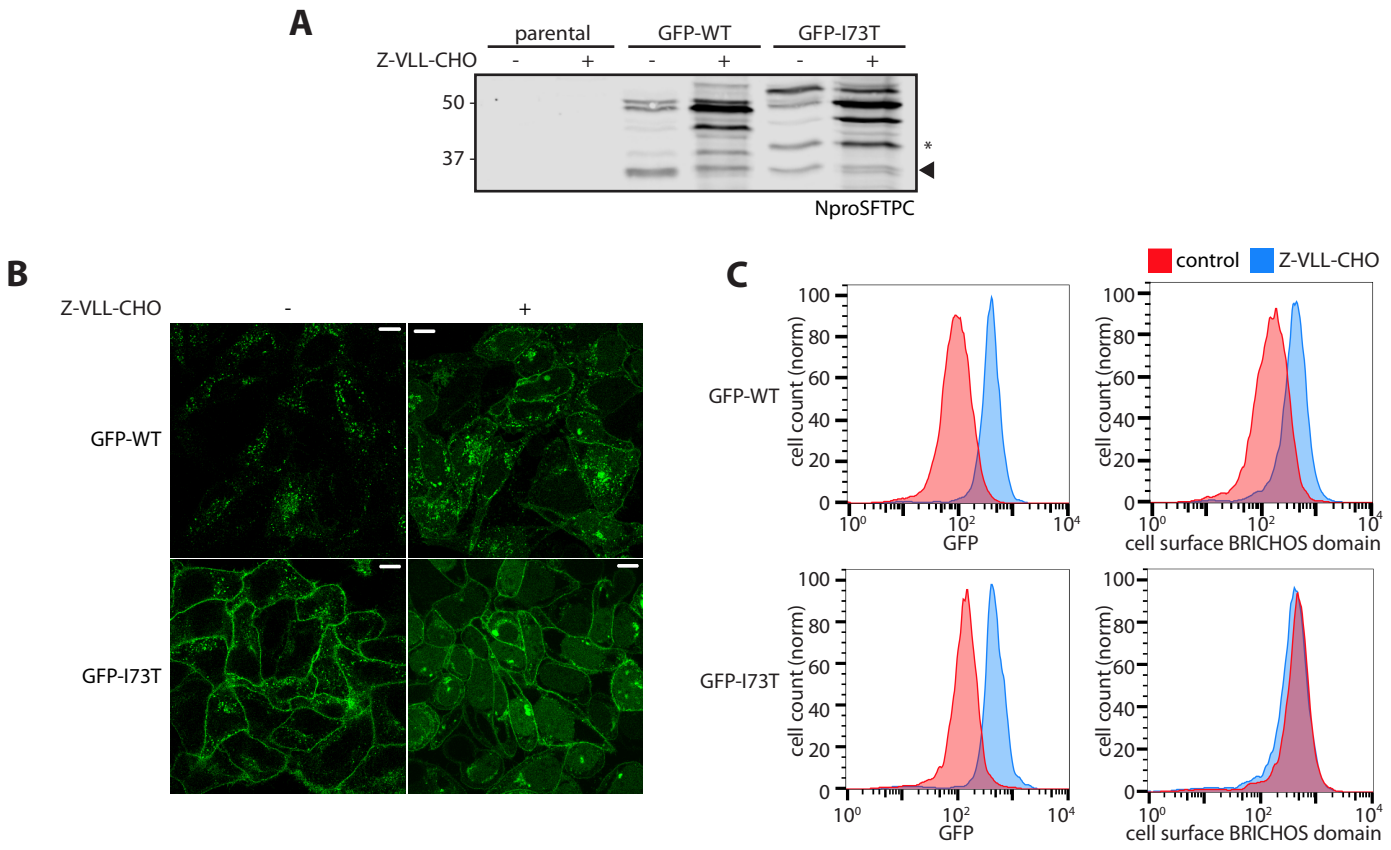

Fig 7. SFTPC C-terminal cleavage is inhibited by Z-VLL-CHO. (A) HeLa cells stably expressing GFP-SFTPC-WT or I73T were treated with 5μM Z-VLL-CHO for 16hrs and lysates immunoblotted for NproSFTPC. Cells treated with Z-VLL-CHO develop an excess of early C-terminal processing intermediates, increased overall SFTPC (as measured by GFP) and redistribution of SFTPC to the plasma membrane as seen by confocal microscopy (B) and flow cytometry (C). Scale bar = 10μm.

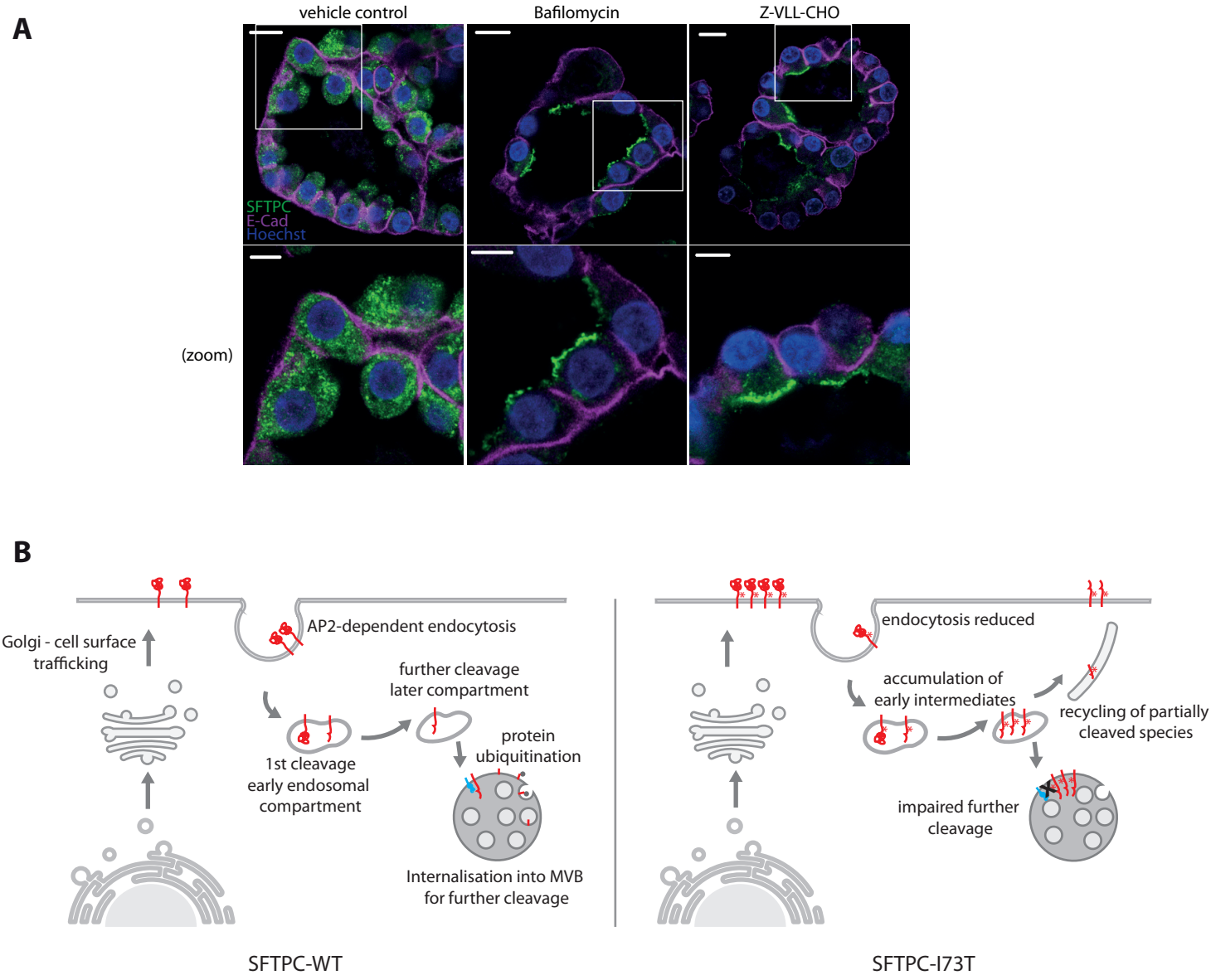

Fig 8. SFTPC is trafficked via the cell surface in human alveolar organoids. (A) Human AT2 cell organoids were treated with bafilomycin or Z-VLL-CHO and the localisation of SFTPC determined by immunohistochemistry. E-cadherin (E-Cad) was used to delineate the basolateral membranes. Note that both compounds redistribute SFTPC to the apical plasma membrane. Scale bar = 10μm / 5μm (zoomed images). (B) Proposed model of SFTPC trafficking. SFTPC pro-protein is trafficked to the plasma membrane from the Golgi before AP2 dependent endocytosis in clathrin coated vesicles. Initial C-terminal cleavage occurs in an early endocytic compartment before further cleavage in a later compartment by a membrane protease. This facilitates ubiquitination and allows internalisation into MVBs for onward cleavage and packaging into lamellar bodies. In the presence of the I73T mutation, endocytosis is reduced, early intermediates accumulate and are recycled due to a later block in trafficking mediated by failure of later cleavage, ubiquitination and MVB internalisation.

Supplementary Materials and Methods

Chemical reagents

The following chemicals were used: Bafilomycin (Sigma B1973) – 100µM stock solution in DMSO, working concentration 100nM; Z-VLL-CHO (Abcam Ab146640) - 10mM stock solution in DMSO, working concentration 5µM; proteinase K (Sigma p7850).

Antibodies

The following commercial antibodies were used: Npro SFTPC (Abcam Ab90716 / Santa Cruz SC-7706); BRICHOS domain SFTPC (Abgent AP13684b); HA tag (Cell Signalling SC3724); GFP (Abcam Ab1218); Ubiquitin (Cayman Chemical FK2); transferrin receptor (TfnR) (BD bioscience BD-555534); cation-dependent mannose -6-phosphate receptor (CDMPR) (Ab2733); MICAL-L1 (Novus H00085377); GGA3 (BD Bioscience BD612310); AP2 (Novus NB300-721); Ube2N (Abcam Ab109286); HLA (Abcam Ab134189); actin (Abcam Ab3280); GAPDH (Cell signalling 2118 / Merk Millipore MAB374); HTII-280 (Terrace Biotech TB-27AHT2-280); E-cadherin (BD Bioscience BD610182). The Hrs, GGA1 and GGA2 antibodies were kind gifts from the Robinson lab (Cambridge, UK) [1]. The following secondary antibodies were used: IRdye 680/800CW anti-rabbit/mouse 680/800 (LiCor); donkey/ goat anti mouse/ rabbit/ goat AF405/488/594/647 conjugated antibodies (Invitrogen).

Expression vectors

pcDNA-SFTPC, pcDNA-HA-SFTPC and peGFP-SFTPC WT/I73T expression vectors were kind gifts from Professor Mike Beers [2]. The K6R and I73A variants were derived by site directed mutagenesis. HaloTag®-SFTPC, peGFP-SFTPC-linker-HaloTag and internally tagged SFTPC constructs were made either by Gibson assembly or by PCR using oligonucleotides incorporating tag sequences. The Str-KDEL_TfnR-SBP-mCherry/CD-MPR-SBP-mCherry plasmids were a kind gift from David Gershlick (Cambridge, UK) [3]. The Str-Ii_SBP-eGFP-SFTPC constructs were made by Gibson assembly using the Str-Ii_SBP-eGFP-Golgin84 starting plasmid (Addgene 65303). Vectors for CRISPR/Cas9 gene editing were generated using the Zhang protocol[4]. A suitable Ube2N guide sequence was selected from the Brunello library [5] (CCTCAAAGGGGGAATCCTGA) and cloned into the pSpCas9(BB)-2A-mCherry vector which was a kind gift from the Ron lab (Cambridge, UK) [6].

Cell lines and siRNA

mStrawberry-Rab8 HeLa cells, originally made by Andrew Peden (Sheffield, UK) were a kind gift from Matthew Seaman (Cambridge, UK) [7]; The AP2 knockout HeLa pool were a gift from the Bonifacino lab (NIH, USA) [3] and GGA2 knock-sideways HeLa cells a gift from the Robinson lab (Cambridge, UK) [8]. siRNAs (Dharmacon) were introduced by reverse transfection using RNAiMAX (Thermofisher) for 24 hours before refreshing the media: Hrs (UUUACCUCCACUUGUCUCUdTdT); GGA1 (J-013694-08; CACAGGAGUGGGAGGCGAU); GGA2 (J-012908-11; UGAAUUAUGUUUCGCAGAA); GGA3 (J-012881-11; UGUGACAGCCUACGAUAAA). Control siRNA was acquired from Ambion (Texas, USA).

Western blotting and immunofluorescence

Triton lysis, SDS-PAGE electrophoresis followed by immunoblotting and immunofluorescence of immortalised cells were performed as previously described [9] [10].

Paraffin embedded tissue was deparaffinised and rehydrated using xylene (3x5min) and EtOH (2 minutes each of 100%, 70%, 50%, 0%) then antigen retrieval undertaken by boiling in 10mM sodium citrate, 0.05% tween20 pH 6.0 for 10 minutes. Samples were blocked with 1% BSA then incubated overnight with primary antibody at 4°C then secondary antibody diluted 1:500 for 1 hour at room

temperature. Hoechst (Invitrogen) 1:5000 was added to the penultimate wash before mounting with Prolong Gold Antifade (Thermofisher).
Blots were developed using a LiCor Odyssey and all imaging undertaken on an LSM880 confocal microscope.

Immunoprecipitation
Briefly, for SFTPC immunoprecipitation 30µl Sepharose A bead slurry (Lifetech 10-1041) were bound to a 2µl non-specific Rb IgG (Ab37415) or 1µg SFTPC Ab (Ab90716) per sample for 1 hour at 4°C. Cells were lysed in 1% Triton lysis buffer before normalised amounts of protein were precleared then transferred to the IP beads and incubated overnight at 4°C. Protein was eluted into SDS loading buffer. GFP-Trap®-magnetic agarose beads (Chromotek) were used following the manufacturer's protocol and the recommended 0.5% NP-40 lysis buffer. Samples were incubated with beads for 1 hour before washing in RIPA buffer to minimise non-specific binding.

Proteinase K assay
HeLa cells stably expressing GFP-SFTPC-WT or GFP-SFTPC-I73T were resuspended in PBS with calcium/magnesium. Proteinase K (Sigma p7850) was added on ice for 1 hour then inhibited with 5mM PMSF before proceeding to cell lysis.

O-Glycosylation assay
Lysates from cells stably expressing GFP-SFTPC-WT or GFP-SFTPC-I73T were heated with 1x New England Biolabs (NEB) glycoprotein denaturing buffer to 100°C for 10 minutes the treated with neuraminidase (NEB 0720) or O-glycosidase (NEB 0733) at 37°C for 4 hours in appropriate NEB buffers.

Flow cytometry
Cells were detached using 10mM EDTA, washed with cold PBS, blocked with 10% FBS for 30 minutes then incubated with the relevant primary antibody (30 minutes at 4°C) and AF647-conjugated secondary (30 minutes at 4°C). Cells were fixed with 4% PFA then analysed with a BD FACSCalibur and FlowJo, normalising results to the mode. For the quantitative antibody feeding assay, cells were detached using EDTA and resuspended in ice cold media for labelling with primary antibody on ice for 30 minutes. Cells were pelleted and washed with ice cold PBS before being aliquoted and resuspended in cold media. Cold media was replaced with warmed media at the point of returning samples to the incubator for the indicated time periods. At the end of internalisation cells were placed back on ice, washed with cold PBS and incubated with AF647-conjugated secondary antibody at 4°C for 30minutes. Cells were washed again with cold PBS then fixed with 4% PFA and analysed.

Live cell assays and imaging
Imaging was undertaken on an LSM880 confocal microscope or Zeiss Airyscan using Zen black software.
RUSH imaging: Cells were transfected with 2.5µg RUSH vectors 48 hours before imaging. 585µM biotin was added to warm tissue culture media and used to replace the media. For real-time video imaging, a 2x biotin stock was prepared in warm culture media which was added to cells *in situ* before imaging.
Knocksideways assays: GGA2-mito HeLa cells were transfected with 10nM siRNA GGA1-3, incubated for 24 hours then transfected with 3µg SBP-GFP-SFTPC RUSH vectors. 48 hours after transfection, cells were treated ± 200nM rapamycin to knock GGA2 sideways, then treated ± 585µM biotin for 2 hours before fixing and imaging.

HaloTag labelling: Cells expressing HaloTag fusion proteins were labelled using TMR ligand (Promega) diluted 1:5000 for 10 minutes, washed x3 with media, incubated for 30minutes then fixed and imaged.

Antibody feeding was undertaken by incubating live cells grown on coverslips with the relevant primary antibody diluted in tissue culture media on ice, typically for 30 minutes followed by washing with ice cold PBS. For microscopy, labelled cells were transferred to 37°C for the indicated times before being placed back on ice, then fixed with 4% PFA but not permeabilised. Remaining cell surface protein was labelled with an AF405-conjugated secondary before permeabilising and blocking with 0.1% Triton-X + 10% FBS. An AF594-conjugated antibody was then used to label internalised protein before being washed, stained with DAPI (1:1000 in PBS) and mounted.

Mass spectrometry

Lysates from GFP-SFTPC-expressing HeLas were subjected to anti-GFP immunoprecipitation and eluates separated by SDS-PAGE electrophoresis. Bands were excised, subjected to trypsin digest and run on a Q Exactive Plus spectrometer. Data were processed using PEAKS Studio (version 8.0, Bioinformatics Solutions Inc.) and PTM coverage images exported from the results of the PEAKS Spider stage. A custom R script plotted the coverage of each residue as a percentage of total protein coverage, weighted taking into account the relative abundance (area under the curve) for each peptide. The horizontal dashed line (fig s1C) represents predicted even coverage.

References

1. Hirst J, Lui WW, Bright NA, Totty N, Seaman MN, Robinson MS. A family of proteins with gamma-adaptin and VHS domains that facilitate trafficking between the trans-Golgi network and the vacuole/lysosome. *J Cell Biol* 2000: 149(1): 67-80.
2. Beers MF, Hawkins A, Maguire JA, Kotorashvili A, Zhao M, Newitt JL, Ding W, Russo S, Guttentag S, Gonzales L, Mulugeta S. A nonaggregating surfactant protein C mutant is misdirected to early endosomes and disrupts phospholipid recycling. *Traffic* 2011: 12(9): 1196-1210.
3. Chen Y, Gershlick DC, Park SY, Bonifacino JS. Segregation in the Golgi complex precedes export of endolysosomal proteins in distinct transport carriers. *J Cell Biol* 2017: 216(12): 4141-4151.
4. Ran FA, Hsu PD, Wright J, Agarwala V, Scott DA, Zhang F. Genome engineering using the CRISPR-Cas9 system. *Nat Protoc* 2013: 8(11): 2281-2308.
5. Doench JG, Fusi N, Sullender M, Hegde M, Vaimberg EW, Donovan KF, Smith I, Tothova Z, Wilen C, Orchard R, Virgin HW, Listgarten J, Root DE. Optimized sgRNA design to maximize activity and minimize off-target effects of CRISPR-Cas9. *Nat Biotechnol* 2016: 34(2): 184-191.
6. Amin-Wetzel N, Saunders RA, Kamphuis MJ, Rato C, Preissler S, Harding HP, Ron D. A J-Protein Co-chaperone Recruits BiP to Monomerize IRE1 and Repress the Unfolded Protein Response. *Cell* 2017: 171(7): 1625-1637 e1613.
7. Breusegem SY, Seaman MNJ. Genome-wide RNAi screen reveals a role for multipass membrane proteins in endosome-to-golgi retrieval. *Cell Rep* 2014: 9(5): 1931-1945.
8. Hirst J, Borner GH, Antrobus R, Peden AA, Hodson NA, Sahlender DA, Robinson MS. Distinct and overlapping roles for AP-1 and GGAs revealed by the "knocksideways" system. *Curr Biol* 2012: 22(18): 1711-1716.
9. Malzer E, Szajewska-Skuta M, Dalton LE, Thomas SE, Hu N, Skaer H, Lomas DA, Crowther DC, Marciniak SJ. Coordinate regulation of eIF2alpha phosphorylation by PPP1R15 and GCN2 is required during Drosophila development. *J Cell Sci* 2013: 126(Pt 6): 1406-1415.
10. Dickens JA, Ordonez A, Chambers JE, Beckett AJ, Patel V, Malzer E, Dominicus CS, Bradley J, Peden AA, Prior IA, Lomas DA, Marciniak SJ. The endoplasmic reticulum remains functionally connected by vesicular transport after its fragmentation in cells expressing Z-alpha1-antitrypsin. *FASEB J* 2016: 30(12): 4083-4097.

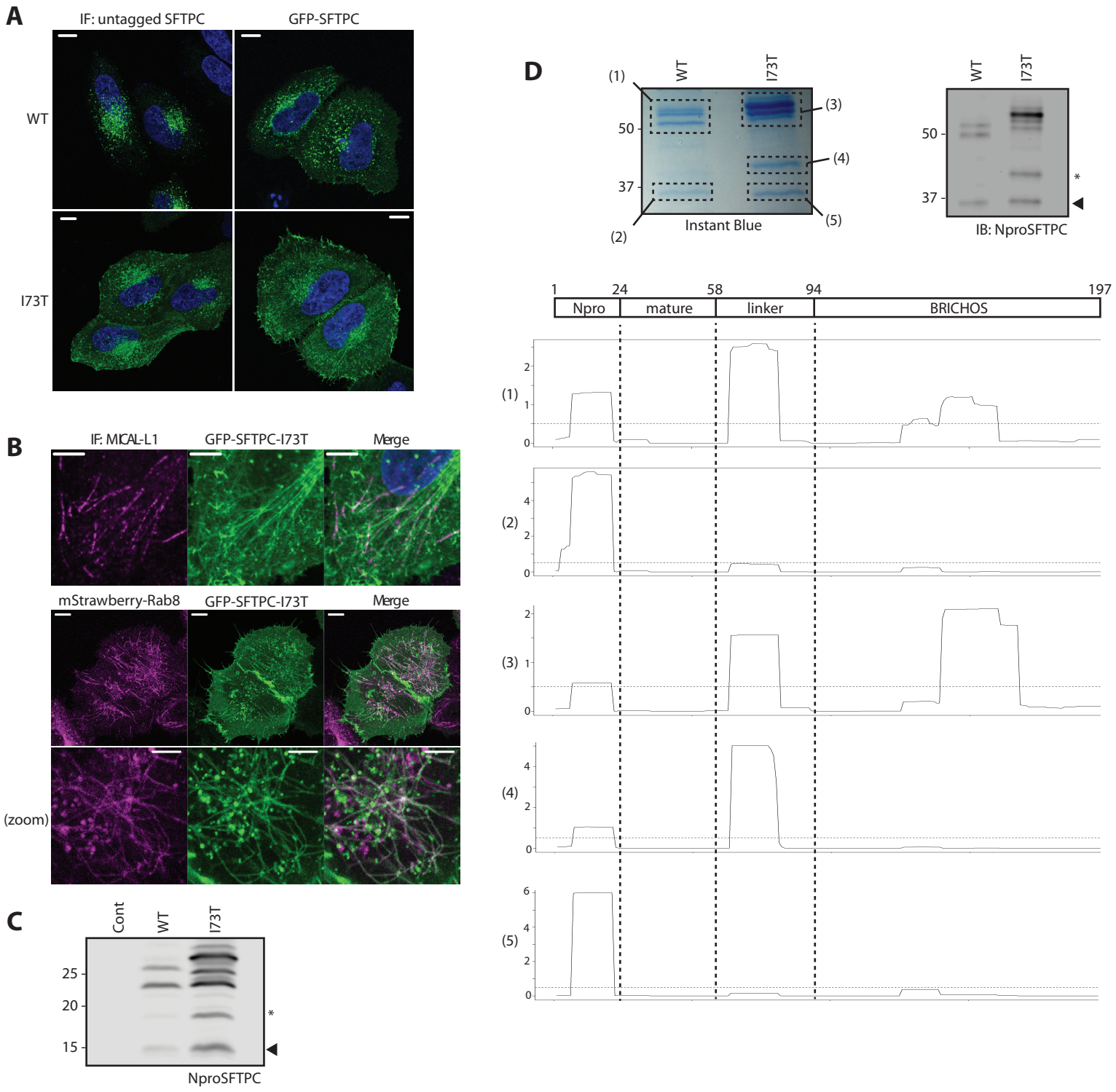

Suppl fig 1. Characterisation of SFTPC expression and cleavage in an immortalised cell system. (A) Confocal imaging of immunostained untagged SFTPC and GFP-SFTPC localisation in HeLa cells. Addition of the GFP tag did not alter the localisation of SFTPC-WT and I73T. (B) Intracellular tubular structures in cells expressing SFTPC-I73T are confirmed as recycling endosomes due to co-localisation with MICAL-L1 (upper panels) and mStrawberry-Rab8 (lower panels). (C) Untagged SFTPC or vector control were transiently expressed in HeLa cells and lysates immunoblotted using an N-terminal SFTPC antibody. (D) Mass spectrometry analysis confirms the aberrant intermediate seen for SFTPC-I73T is partially cleaved but retains the linker region. Pooled lysates from HeLa cells stably expressing GFP-SFTPC-WT and I73T were subjected to anti-GFP immunoprecipitation. Eluates were separated by SDS-PAGE (upper L panel) and relevant bands confirmed by immunoblot (upper R panel). Fragments obtained by trypsin digest were subjected to mass spectrometry. Good coverage was obtained except for the very hydrophobic transmembrane domain. Data displayed as coverage of each residue as a percentage of total protein coverage. Scale bar = 10µm / 5µm (zoomed images).

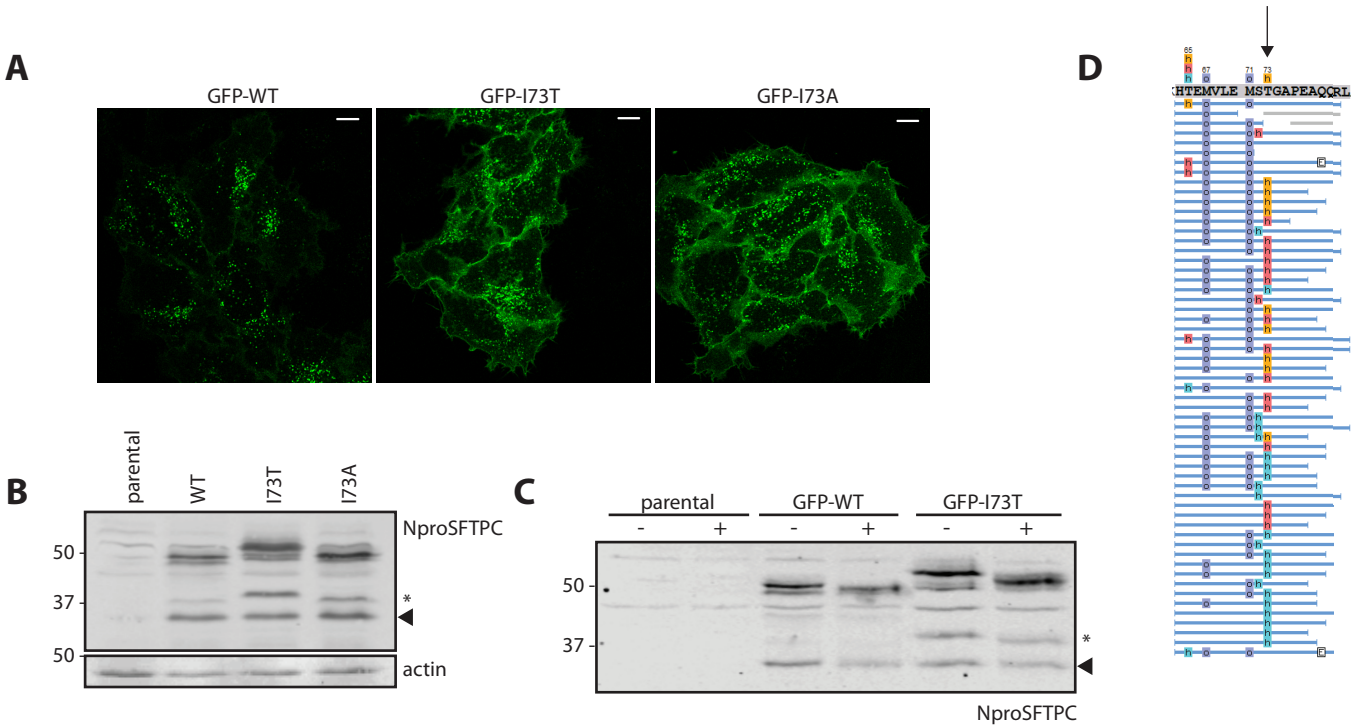

Suppl fig 2. SFTPC I73T is O-glycosylated on T73 but it is the loss of I73, not gain of T73, that causes aberrant trafficking. GFP-SFTPC WT, I73T and I73A were transiently expressed in HeLa cells. Their subcellular localisation was assessed by confocal microscopy (A) and cleavage pattern by immunoblot (B). Note that the loss of I73 determines the mistrafficking phenotype but it is the gain of T73 that alters the band size of full length and early processing intermediates. (C) Immunoblots of HeLa cell lysates following treatment with O-glycosidase revert the band pattern of GFP-SFTPC-I73T to that more similar to GFP-SFTPC-WT. (D) Lysates from HeLa cells expressing GFP-SFTPC-I73T were subjected to GFP-trap immunoprecipitation, separated by protein gel electrophoresis and GFP-SFTPC-I73T bands extracted and subjected to mass spectrometry analysis. Resulting fragments confirm O-glycosylation of T73 ("h" annotation). Scale bar = 10µm.

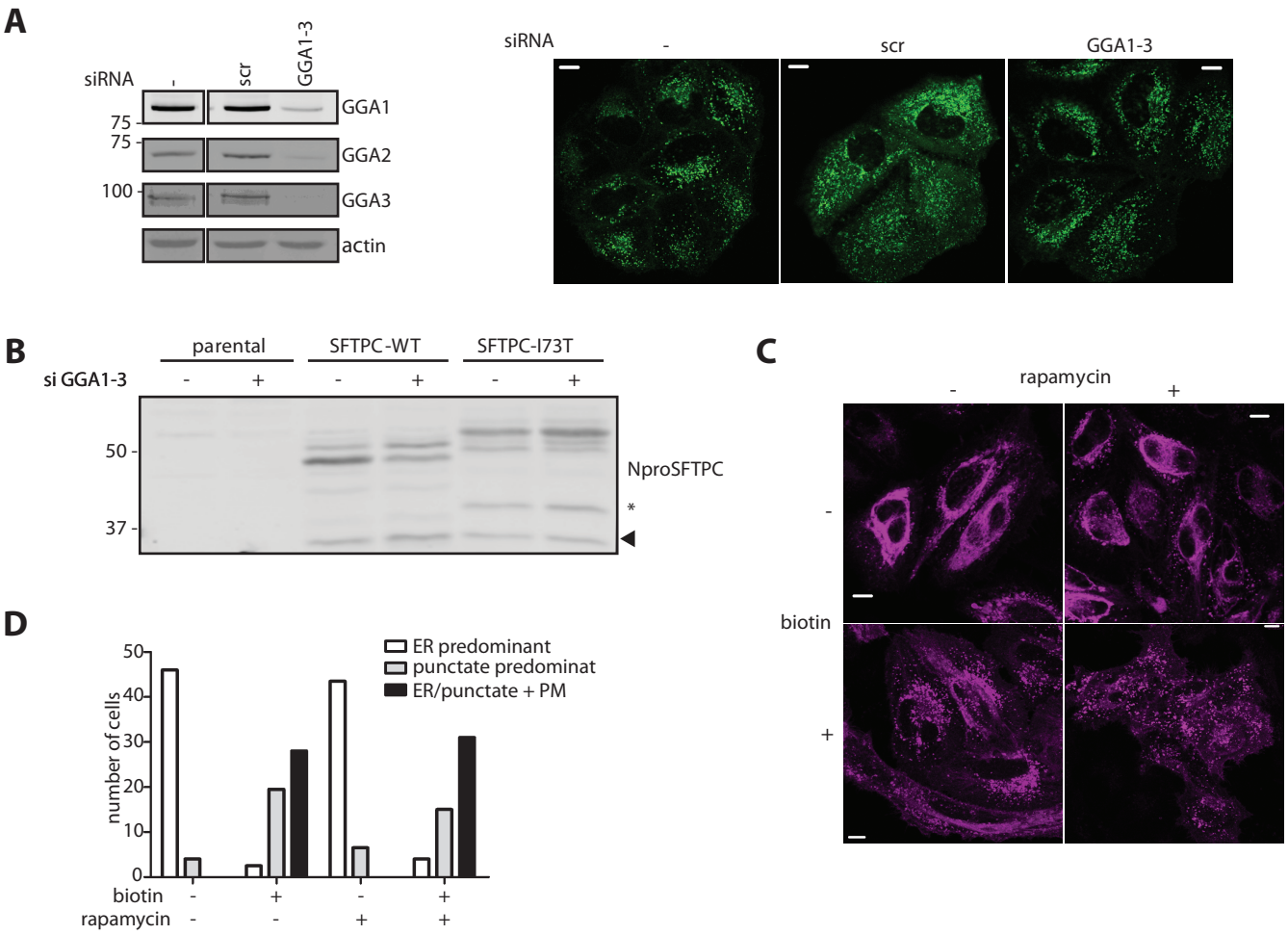

Suppl fig 3. Depletion of GGA proteins does not affect SFTPC trafficking. (A) siRNAs were used to deplete GFP-SFTPC-WT-expressing cells of GGA proteins 1-3, confirmed by immunoblot. The subcellular localisation of SFTPC-WT does not change with knockdown, and nor does the post translational cleavage as measured by immunoblot (B). (C) To mitigate for cellular adaptation to GGA knockdown, a knock sideways system was used. GGA2 was knocked down in GGA2 knocksideways HeLa cells before transfection with GFP-SFTPC-WT RUSH vectors. SFTPC was allowed to traffic by addition of biotin in the presence or absence of GGA2 knocksideways. GGA2 knocksideways does not change SFTPC distribution. Quantification in (D). PM = plasma membrane. Scale bar = 10µm.

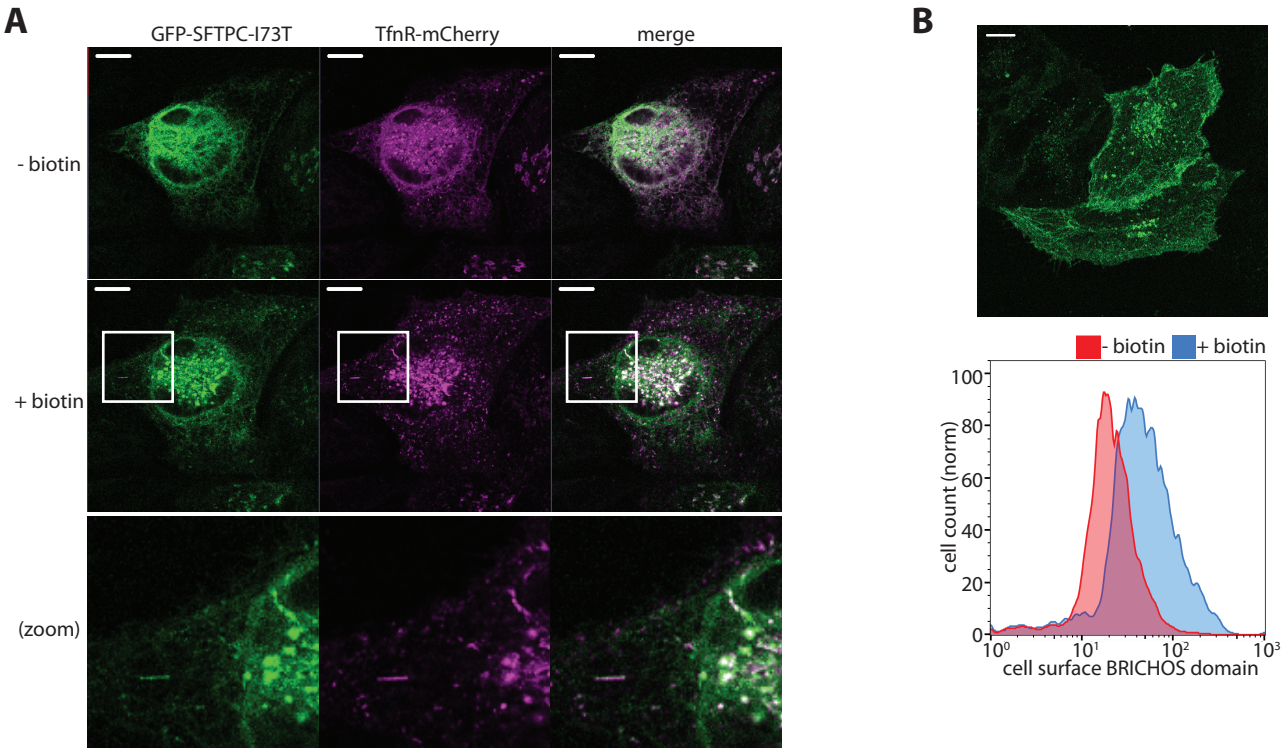

Suppl fig 4. SFTPC-I73T, like SFTPC-WT is trafficked to the plasma membrane from early compartments. (A) GFP-SFTPC-I73T RUSH vectors were co-expressed with TfnR-mCherry and treated with biotin before imaging in real time. Like SFTPC-WT, GFP-SFTPC-I73T traffics with TfnR in tubular structures. (B) After 2 hours of biotin exposure, GFP-SFTPC-I73T is visible at the plasma membrane; this is reflected in increased BRICHOS domain presence at the plasma membrane by flow cytometry. Scale bar = 10µm.

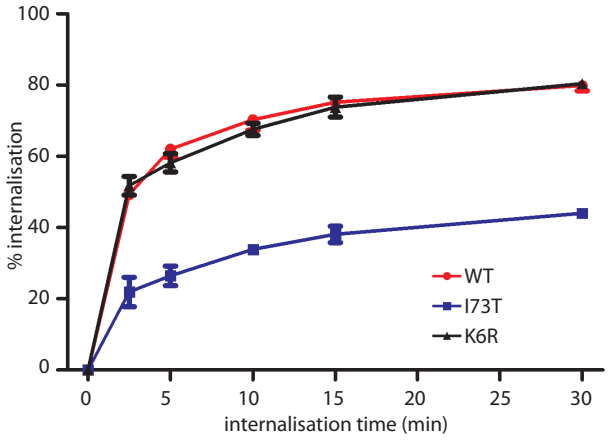

Suppl fig 5. Addition of a GFP tag does not affect SFTPC endocytosis. Quantitative SFTPC internalisation assay. Cells expressing untagged SFTPC-WT, I73T or K6R were labelled with BRICHOS domain antibody on ice, then protein allowed to internalise at 37°C for the indicated times. Cells were placed back on ice, fixed but not permeabilised, and labelled with a secondary antibody before analysis by flow cytometry. n=3, mean +/- sem.

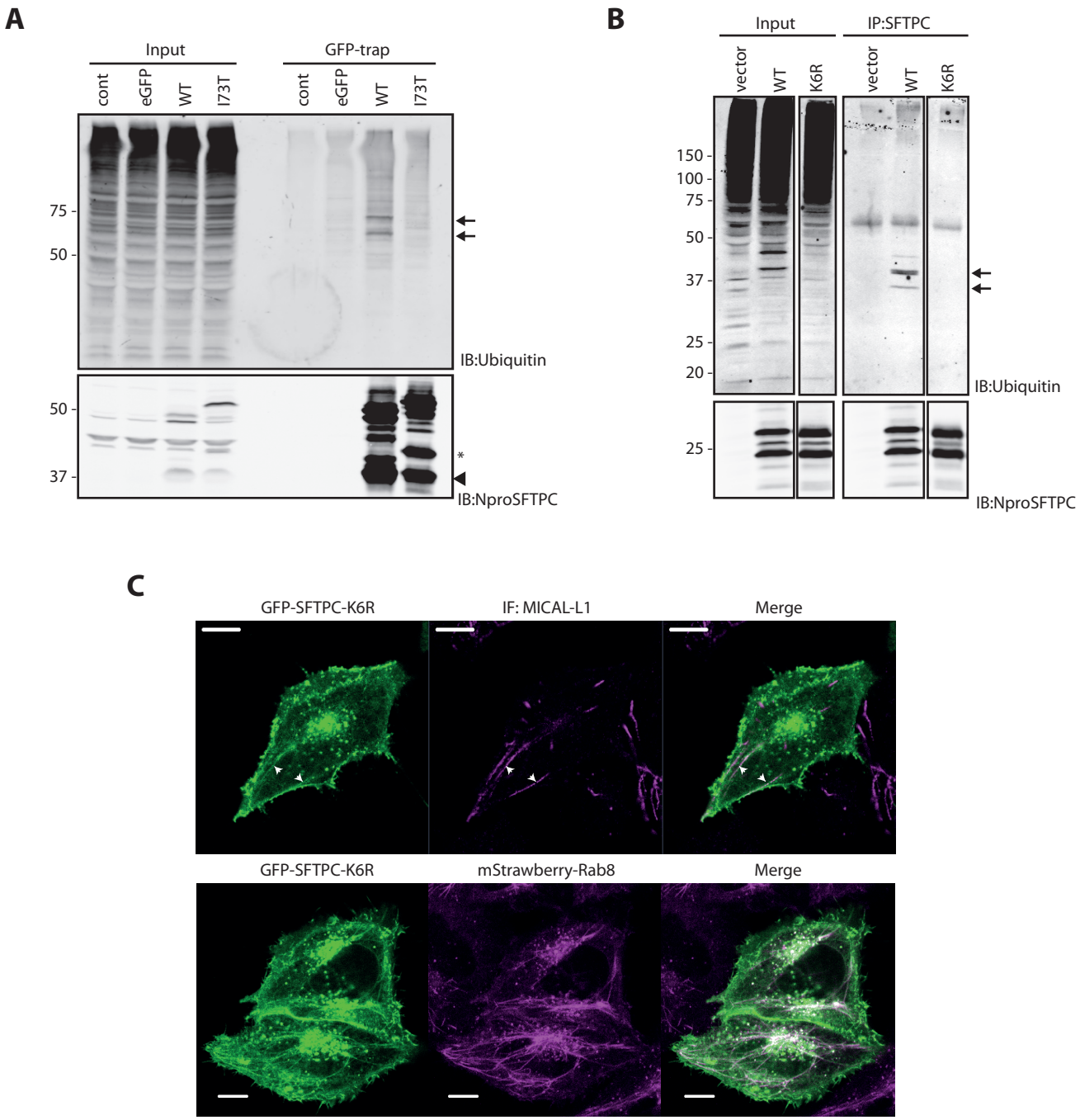

Suppl fig 6. GFP-SFTPC-I73T and K6R fail to be ubiquitinated. (A) Lysates from HeLa cells transfected with vector control, eGFP or GFP-SFTPC were subjected to GFP immunoprecipitation and immunoblotted for ubiquitin and SFTPC. Note the presence of oligoubiquitinated SFTPC-WT (arrows) which is not seen in I73T-expressing cells. (B) Lysates from HeLa cells transfected with vector control, SFTPC-WT or ubiquitination site mutant K6R were subjected to SFTPC immunoprecipitation and immunoblotted for ubiquitin and SFTPC. Note the presence of oligoubiquitinated SFTPC-WT (arrows) which is not seen in the presence of the K6R mutation. (C) Intracellular tubular structures in cells expressing SFTPC-K6R are confirmed as recycling endosomes due to co-localisation with MICAL-L1 (upper panels) and mStrawberry-Rab8 (lower panels). Scale bar = 10μm.

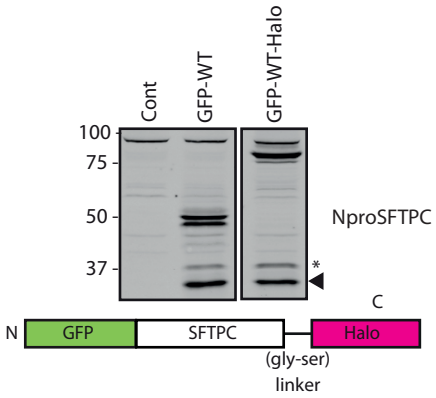

Suppl fig 7. Addition of a C-terminal Halotag does not affect SFTPC cleavage. HeLa cells were transfected with a vector control, GFP-SFTPC or GFP-SFTPC-Halo and lysates immunoblotted for SFTPC. This confirmed that addition of the C-terminal Halotag does not affect post translational cleavage.

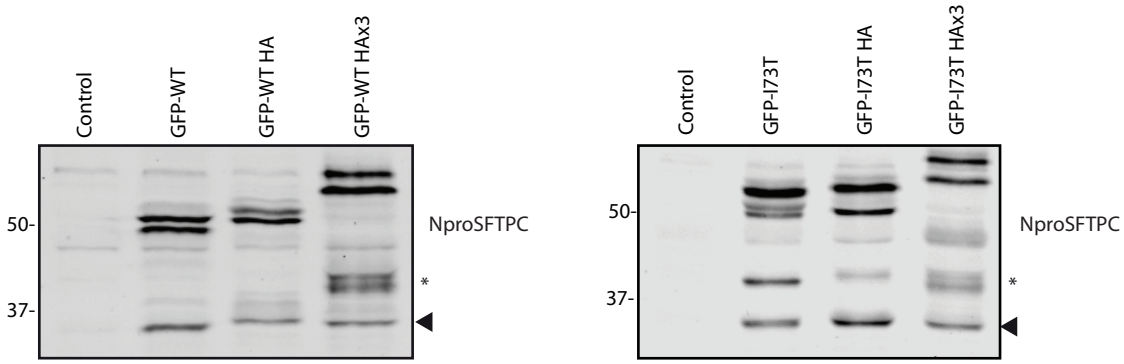

Suppl fig 8. Alteration of the proximal linker region's length with an internal tag affects cleavage. A vector control, one or three HA tags were introduced into the juxta-membrane linker region of GFP-SFTPC (L panel) or I73T (R panel). Expression of these constructs resulted in accumulation of a processing intermediate (*), more marked for SFPTC-WT, consistent with impaired cleavage at the membrane.